

Talbot HM, Bischoff J, Inglis GN, Collinson ME, Pancost RD.

[Polyfunctionalised bio- and geohopanoids in the Eocene Cobham Lignite.](#)

Organic Geochemistry 2016

DOI: <http://dx.doi.org/10.1016/j.orggeochem.2016.03.006>

Copyright:

© 2016. This manuscript version is made available under the [CC-BY-NC-ND 4.0 license](#)

DOI link to article:

<http://dx.doi.org/10.1016/j.orggeochem.2016.03.006>

Date deposited:

18/03/2016

Embargo release date:

19 September 2017



This work is licensed under a

[Creative Commons Attribution-NonCommercial-NoDerivatives 4.0 International licence](#)

Polyfunctionalised bio- and geohopanoids in the Eocene Cobham Lignite

Helen M. Talbot^{a,*}, Juliane Bischoff^a, Gordon N. Inglis^b, Margaret E. Collinson^c and Richard D. Pancost^b

^a*School of Civil Engineering and Geosciences, Newcastle University, Newcastle upon Tyne, NE1 7RU, UK.*

^b*Organic Geochemistry Unit, The Cabot Institute and Bristol Biogeochemistry Research Centre, School of Chemistry, University of Bristol, Bristol BS8 1TS, UK.*

^c*Department of Earth Sciences, Royal Holloway University of London, Egham, Surrey TW20 0EX, UK.*

Keywords: Cobham Lignite, peat, PETM, methanotrophy, bacteriohopanepolyols, aminobacteriohopanepentol, anhydrobacteriohopanetetrol

** Corresponding author. Tel.: +44 (0)191 208 6426*

E-mail address: helen.talbot@ncl.ac.uk (H. M. Talbot).

Abstract

We investigated the bacteriohopanepolyol (BHP) distribution in the Cobham Lignite sequence (SE England) deposited across the Palaeocene-Eocene boundary including part of the Palaeocene-Eocene Thermal Maximum (PETM) as shown previously by a negative carbon isotope excursion (CIE). A variety of BHPs were identified, including the commonly occurring and non-source specific biohopanoid bacteriohopanetetrol (BHT) and 32,35-anhydroBHT which was the most abundant polyfunctionalised geohopanoid in the majority of samples. BHPs with a terminal amine functionality, diagnostic biomarkers for methanotrophic bacteria were identified throughout the sequence, with similar distributions in both the lower laminated and upper blocky lignite except that 35-aminobacteriohopanepentol (aminopentol) indicative of Type I methanotrophs (gammaproteobacteria) was generally more abundant in the upper section within the CIE.

The diagenetic fate of these compounds is currently poorly constrained, however, we also identified the recently reported N-containing transformation product anhydroaminotriol and several tentatively assigned novel N-containing structures potentially containing ketone functionalities. Although present throughout the section, there is a sharp peak in the occurrence of these novel compounds correlated with the onset of the CIE and highly isotopically depleted hopanes in the upper part of the laminated lignite, both also correlate well with peak abundance of aminopentol. The significant abundance of these compounds suggests that 35-amino BHPs have their own specific diagenetic pathway, potentially providing an alternative method allowing methanotroph activity to be traced in older samples even if the original biohopanoid markers are no longer present.

At this time we cannot preclude the possibility that some or all of these BHPs have been produced by more recent subsurface activity, post deposition of the lignite to date; however, that would not be expected to generate the observed stratigraphic variability and we suggest that unprecedented observations of a range of highly functionalised biohopanoids in samples of this age could significantly extend the window of their known occurrence.

1. Introduction

Bacteriohopanepolyols (BHPs) are highly functionalised pentacyclic triterpenoids derived from a wide range of prokaryotes (e.g. Rohmer et al., 1984; Pearson et al., 2007, 2009). In their biological form (i.e. biohopanoids), they comprise a diverse suite of structures (e.g. Rohmer, 1993; See Appendix for examples) which have been linked to cellular membrane adaptation, regulating fluidity and permeability in response to environmental stress (e.g. Kannenberg and Poralla, 1999; Welander et al., 2009; Sáenz et al., 2012; Kulkarni et al., 2013). Typically they contain four, five or six functional groups (termed tetra-, penta- and hexafunctionalised respectively) at the C-30 to 35 positions of the side chain although cyclised side chains are also known. For example, adenosylhopane (**lp**) is the precursor for all other side chain extended BHPs (Bradley et al., 2010) via a pathway involving the intermediate ribosylhopane (Liu et al., 2014; Bodlenner et al., 2015). Biohopanoids are also the precursors of the ubiquitous geohopanoids (hopanols, hopanoic acids, hopanes) found in geological materials (e.g. Ourisson et al., 1987; Ourisson and Albrecht, 1992; Farrimond et al., 2004).

Biohopanoids can provide useful information about certain source organisms, biogeochemical processes and environmental conditions (e.g. Talbot and Farrimond, 2007). One such group are BHPs with an amine functionality at the C-35 position (collectively termed aminoBHPs herein; e.g. Talbot et al., 2014; Wagner et al., 2014; Spencer-Jones et al., 2015) which include 35-aminobacteriohopane-32,33,34-triol (aminotriol from herein, **lf**), 35-aminobacteriohopane-31,32,33,34-tetrol (aminotetrol, **lg**) and 35-aminobacteriohopane-30,31,32,33,34-pentol (aminopentol, **lh**). Sources of aminopentol are thought to be restricted to Type I aerobic methane oxidising bacteria (Gammaproteobacteria; e.g. Neunlist and Rohmer, 1985; Cvejic et al., 2000; van Winden et al., 2012a), whilst aminotetrol is produced

by both Type I and II (Alphaproteobacteria) methanotrophs. The only known additional source of the penta- and hexafunctionalised compounds are some species of *Desulfovibrio* sulphate reducing bacteria (SRB; Blumenberg et al., 2006, 2009), although aminopentol was only reported from one species at trace levels (Blumenberg et al., 2012). Further, when observed in *Desulfovibrio* sp., the ratio of aminotriol to aminotetrol (**lf/lg**) was in the range of 20 to 100 (Blumenberg et al., 2006, 2009, 2012) whilst it is significantly lower in most methanotrophs, with the pentafunctionalised compound often more abundant (e.g. Janke et al., 1999; Talbot et al., 2001). Aminotriol is less diagnostic as it is produced by a range of other prokaryotes (including other proteobacteria and some cyanobacteria; Talbot et al., 2008 and references therein) in addition to all Type II and some Type I methanotrophs (Talbot et al., 2001; van Winden et al., 2012a; Banta et al., 2015).

AminoBHPs have been reported from a wide range of environments including soils (e.g. Cooke et al., 2008a; Xu et al., 2009; Pearson et al., 2009; Rethemeyer et al., 2010; Kim et al., 2011; Zhu et al., 2011), peats (e.g. van Winden et al., 2012a,b), marine, river and lacustrine sediments (e.g. Talbot et al., 2003a; Talbot and Farrimond, 2007; Coolen et al., 2008; Blumenberg et al., 2010; Zhu et al., 2010, 2011; Blumenberg et al., 2013). Aminotetrol (**lg**) and aminopentol (**lh**) are therefore of particular interest and have been used to identify material sourced from sites of intense aerobic methane oxidation such as river estuaries (Zhu et al., 2010), tropical wetlands (Talbot et al., 2014; Wagner et al., 2014; Spencer-Jones et al., 2015) and water columns (e.g. Blumenberg et al., 2007; Wakeham et al., 2007; Berndmeyer et al., 2013). Other markers for Type I aerobic methanotrophs include hopanoids methylated at the C-3 position (e.g. Cvejic et al., 2000), but non-methanotrophs can also be potential sources of this structural feature (e.g. Welander and Summons, 2012). Typically therefore, these studies also rely on analysis of compound specific carbon isotope ratios with strong isotopic depletion expected for methanotroph-derived lipids (e.g. Collister et al., 1992). However, the absence of C-3 methylated pseudohomologues of these aminoBHP compounds does not preclude either the Type II methanotrophs or Type I

organisms such as *Methylomonas* sp. or *Methylovulum* sp. (e.g. Rohmer et al., 1984; van Winden et al., 2012a) which do not produce the methylated homologues (see discussion in Talbot et al., 2014).

Originally considered to be rapidly transformed to geohopanoids at the earliest stages of diagenesis (both free and bound), evidence is now growing that polyfunctionalised biohopanoids may be more stable than originally thought. The oldest reported polyfunctionalised biohopanoid is bacteriohopane-32,33,34,35-tetrol (BHT; **1c**) in a sample of marine Palaeogene cores from Tanzania dating to 50.4-49.7 million years ago (Ma; van Dongen et al., 2006). This compound is the most frequently reported BHP structure, facilitated by the fact that it is amenable to analysis by gas chromatography mass spectrometry (GCMS) as well as liquid chromatography mass spectrometry (LCMS; e.g. Talbot et al., 2003a). It has a wide range of potential prokaryotic sources meaning that it cannot be considered as indicative of any particular group of bacteria or set of environmental conditions (e.g. Talbot et al., 2008). Additional early degradation products retaining multiple functional groups derived from BHT or more complex precursors such as BHT cyclitol ether (**1m**) or BHT glucosamine (**1n**) include 32,35-anhydrobacteriohopane-32,33,34,35-tetrol (anhydroBHT; **1a**) and its C-2 methylated homologue (**1la**; Schaeffer et al., 2008, 2010) and they have been reported in samples up to Jurassic in age (Bednarczyk et al., 2005). Multiple isomers of the related compound derived from a pentafunctionalised precursor i.e. anhydrobacteriohopanepentol (anhydroBHPentol; **1d**) have been reported from geothermal sinters (Talbot et al., 2005; Gibson et al., 2014).

Recently we have identified aminoBHPs including aminopentol (**1h**) in samples from the Congo deep-sea fan aged up to 1.2 Ma and the source of the material is proposed as continental wetland environments (Talbot et al., 2014; Spencer-Jones et al., 2015; Spencer-Jones, 2016). Burhan et al. (2002) reported aminotriol from the Be'eri sulfur deposit (Pleistocene age sandstones of the Southwestern Mediterranean Coastal Plain of Israel),

however, it is uncertain if it represents a Pleistocene age signal or one from sub-contemporary bacteria feeding on seeping methane. These findings suggest that BHP compounds produced in aerobic systems can be preserved in the geological record when conditions are favourable and could therefore be useful in examining methane cycling in more ancient settings.

To explore the potential for BHP preservation in ancient sediments, we investigated the BHP signature of a well preserved, immature lignite sequence from southern England. The Cobham Lignite is an exceptional example of a terrestrial lacustrine/mire deposit associated with the Palaeocene-Eocene thermal maximum (PETM; Collinson et al., 2003, 2007, 2009). Previously, a negative carbon isotope excursion (CIE) indicated by a sharp depletion in $\delta^{13}\text{C}$ of $\sim 1\text{‰}$ in the bulk organic carbon within the section has been interpreted as being the negative CIE characteristic of the PETM onset, although its magnitude is markedly lower than the total extent of the CIE observed in other terrestrial settings (McInerney and Wing, 2011). Furthermore, isotopically light hopanoids have also been reported from this section, suggesting an increase in the methanotroph population resulting from enhanced methane production, likely driven by hydrological changes towards a warmer and wetter climate (Pancost et al., 2007). These changes are also manifested as a lithological change from laminated to blocky lignite. Hopanoids at this site are present in exceptional abundance relative to other biomarkers and are relatively immature based on observation of the biological $17\beta,21\beta(H)$ configuration and lack of compounds with $22S$ stereochemistry (Pancost et al., 2007). We therefore considered this site favourable for investigation of the potential for preservation of polyfunctionalised biohopanoids.

2. Methods

2.1 Site and samples

163

164 The ca. 2 m thick early Paleogene Cobham Lignite sequence used for this study was
165 sampled from a temporary exposure, which became available near Cobham, Kent, southern
166 England, when a cutting was made through a hill for construction of the Channel Tunnel Rail
167 Link during 1999-2000. In order to procure a complete sequence of the lignite with intact
168 stratigraphy, surrounding sediment was excavated to produce pillars (10-15 cm in depth and
169 width) free on three sides. The three exposed sides were enclosed in a plaster jacket to
170 prevent breakage and pillars were removed from the exposure at the fourth side using
171 spades. The fourth side was not enclosed. These plaster-jacketed pillars were stored in
172 ambient room conditions whilst attempts were made to obtain funding for their study.

173 Prior to sub-sampling sediment was removed and discarded from the surface of the exposed
174 side to a depth of c. 3 cm until sediment with original appearance (e.g. colour, degree of
175 integrity) was reached. Sub-sampling of each cleaned pillar was completed within one day.
176 Cleaning and sub-sampling was undertaken using sharp single-edged razor blades that had
177 been rinsed in alcohol and treated in a furnace prior to use. A fresh razor blade was used for
178 each sub-sample. Sub-samples specifically for geochemical analysis were taken from near
179 the centre of the pillar, avoiding the sides. These samples were dried and individually
180 wrapped in aluminium foil, which had previously been treated in a furnace, then transported
181 to the University of Bristol for extraction. The current study utilised aliquots of total lipid
182 extract (TLE) originally prepared by Pancost et al. (2007) and which had been stored dry and
183 frozen (-20°C) until transported to Newcastle in 2012 for BHP analysis.

184 The Cobham Lignite sequence is underlain by a sand and mud unit, beneath which is the
185 late Paleocene Upnor Formation (shallow marine). The Early Eocene Woolwich Shell Beds
186 (marginal marine/lagoonal) overly the lignite. The Woolwich Shell Beds contain the
187 *Apectodinium* acme (Collinson et al., 2009), thus, in combination with the CIE in the upper
188 part of the lower laminated lignite (Pancost et al., 2007), demonstrate that all of the blocky
189 lignite is within the PETM and probably in the early part of the PETM (Collinson et al., 2009).

The site, stratigraphy, lithology, palynology, vegetation change and wetland plant mesofossils have been described in detail elsewhere (Table 1; Collinson et al., 2003, 2007, 2009, 2013; Steart et al., 2007).

The Cobham Lignite sequence includes two thick units of lignite and two thin clay layers. A basal thin pale clay layer (3 cm thick) underlies the lower laminated lignite unit (up to 55 cm thick). The uppermost 25 mm of the lower laminated lignite is transitional and contains thin clay laminae (upper part of Figure 3.3 in Steart et al., 2007). A thicker (up to 10 cm) pale clay layer separates the laminated lignite from the overlying blocky lignite unit (up to 132 cm thick). The bottom of the basal thin pale clay layer is set to 0 cm for the section (Table 1). In total thirty five samples from the original set described by Pancost et al. (2007) were chosen for BHP analysis. The samples ranged from the underlying sand and mud unit through the laminated lignite, middle clay and blocky lignite including samples from the onset of the CIE in the upper laminated lignite (Table 1).

2.2 Extraction and derivatisation

Prior to lipid extraction samples were powdered with a mortar and pestle. The powdered samples were extracted by sonication with a sequence of increasingly polar solvents (four times with dichloromethane (DCM), four times with DCM/methanol (1:1 v/v) and three times with methanol) to produce a total lipid extract (TLE; Pancost et al., 2007).

An aliquot of each TLE was acetylated by adding acetic anhydride and pyridine (1 ml each) and heating at 50 °C for 1 h then left at room temperature overnight to yield acetylated BHPs. The acetic anhydride and pyridine were removed under a stream of N₂. The resulting acetylated extract was dissolved in MeOH/propan-2-ol (3:2, v/v) and filtered through a 0.45 micron PTFE filter, blown down to dryness and redissolved in 500 µl MeOH/propan-2-ol (3:2, v/v) for analysis. Sessions et al. (2013) showed using GCMS analysis that acetylation of

hopanoids can produce anhydroBHT if run for more than 15-30 minutes. However, similar tests on a range of acetylation reagent volumes and reaction times showed no statistically significant variation in concentration or production of anhydroBHT on samples analysed by ion-trap LCMS (Spencer-Jones, 2016).

As no standards were added prior to splitting of the TLE and derivatisation, only relative abundances within individual samples are reported below and are based on LCMS data only.

2.3 Analytical HPLC-APCI-MS

BHPs were measured using reversed-phase HPLC-APCI-MS as described previously (e.g. Cooke et al., 2008a; van Winden et al., 2012a). Compounds were separated using a Thermo Finnigan Surveyor HPLC system equipped with a Phenomenex Gemini C18 5 μ m column (150 mm x 3.0 mm i.d.) and a security guard column of the same material. The flow rate was 0.5 ml/min at 30 °C with the following gradient: 90% A and 10% B (0 min); 59% A, 1% B and 40% C (at 25 min); isocratic (to 40 min), returning to starting conditions over 5 min and stabilizing for 15 min, with A = MeOH, B = water and C = propan-2-ol (all Fisher HPLC grade). The HPLC system was connected to a Thermo Finnigan LCQ ion trap MS instrument equipped with an APCI source operated in positive ion mode. Settings were: capillary temperature 155 °C, APCI vaporiser temperature 400 °C, corona discharge current 8 μ A, sheath gas flow 40 and auxiliary gas 10 (arbitrary units). The instrument was tuned as described previously (Talbot et al., 2003b,c). Detection was achieved at an isolation width of m/z 4.0 and fragmentation with normalised collisional dissociation energy of 30% and an activation Q value (parameter determining the m/z range of the observed fragment ions) of 0.15. LCMSⁿ was carried out in data-dependent mode with three scan events: SCAN 1 – full mass spectrum, range m/z 300–1300; SCAN 2: data-dependent MS² spectrum of the most

intense ion from SCAN 1; SCAN 3: data-dependent MS³ spectrum of the most intense ion from SCAN 2.

For standard runs dynamic exclusion was turned on limiting the number of MS² scans per individual parent ion to 3 before automatically switching to the next most abundant ion.

Where necessary, additional targeted analyses were performed to increase the number of MS² scans per peak. Structures were assigned from comparison with published spectra where possible (Talbot et al., 2003b,c, 2005, 2007a,b) or by comparison of their APCI spectra with those of known compounds as described below.

Although full quantification was not possible, we applied the usual response factors determined previously for BHPs with and without nitrogen where N-containing compounds give an average relative response 1.5 times that of BHPs without a N atom (see van Winden et al., 2012a for details). Furthermore, co elution of aminotriol (**If**) and anhydroaminotriol (**li**) complicates the identification and assessment of the anhydroaminotriol peak area.

Anhydroaminotriol has a base peak [M+H]⁺ of m/z 654. Aminotriol has [M+H]⁺ of m/z 714 but also produces some m/z 654 as well via loss of 1 acetylated functional group (CH₃COOH) which is also seen in the full mass spectrum (SCAN 1). Therefore even when only aminotriol is present there will still be a minor m/z 654 peak. To minimise this effect (i.e. minimise any overestimation of anhydroaminotriol) the relative areas of the m/z 714 and 654 peak in all samples where both are present were compared (Table 1; Column **If/li**). The lowest relative amount of the 654 peak in any sample is equal to 17.9% of the 714 peak area. Therefore 17.9% of the corresponding 714 peak area was subtracted from the m/z 654 peak for each individual sample. The reduced value for the m/z 654 was then used in the calculation of the relative abundance of anhydroaminotriol as a proportion of total BHPs (Table 1).

2.4 GC-MS Analysis

Acetylated hopanepolyols, dissolved in DCM, were analysed by GC-MS using an Agilent 7890A GC split/splitless injector (300°C) linked to an Agilent 5975C MSD (electron energy 70 eV; filament current 220 mA; source temperature 230°C; multiplier voltage 2000V; interface temperature 350°C). A 15 m DB5-HT fused silica column (0.25 mm i.d.; 0.1 mm film thickness) was used with helium as the carrier gas. The oven temperature was programmed from 50 to 200°C at 15°C/min (held for 1 min), from 200 to 250°C at 10 °C/min (held for 1 min) and from 250 to 350°C at 5°C/min (held for 8 min; Talbot et al., 2003a). Hopanoids were identified from full scan (m/z 50–750) analysis of selected samples, by comparison with authentic standards and published spectra and by relative retention times. Additionally, one sample (11.95 cm; Table 1) was analysed in SIM mode targeting ions m/z 191, 205, 391, 405, 449, 493 and 507 (see below).

3. Results

3.1. Identification of polyfunctionalised hopanoids in the Cobham lignite

3.1.1. Biohopanoids

Bacteriohopanetetrol (BHT; **1c**) was present in 26 of the 35 samples and was the only biohopanoid observed in any of the Cobham lignite samples which did not contain an amine at the C-35 position (Fig. 1a, b for example; Table 1). Most samples also contained the common tetrafunctionalised aminotriol (**1f**), typically accompanied by similar relative amounts of the pentafunctionalised aminotetrol (**1g**) (Fig. 2 for example; Table 1). In a smaller number of samples, the hexafunctionalised aminopentol (**1h**, Fig. 2; Table 1) was also observed. These compounds were identified by relative retention time (Fig. 2) and interpretation of APCI mass spectra in comparison to previously published data (Talbot et al., 2003b,c).

3.1.2 AnhydroBHT and related novel hopanoids

The common BHP transformation product anhydroBHT (**1a**) was present in all but one sample and was frequently the most abundant BHP present (Table 1). It is readily identified in the diacetate form via EI mass spectrometry (peak **1a**, Figs. 1b, 3a). Although this spectrum has been published previously (e.g. Bednarczyk et al., 2005), it is included to allow for comparison with a group of related novel components described here for the first time (Fig. 3a).

When analysed by reversed phase HPLC, diacetylated anhydroBHT (**1a**) elutes later than BHT (**1c**), and has an APCI base peak ion of m/z 613 ($= [M+H]^+$; Fig. 1a). The MS² spectrum (Fig. 3b; cf. Talbot et al., 2005) includes major fragments of m/z 553 and 493 indicating 2 neutral losses of 60 Da (i.e. the acetylated OH groups at C-33 and C-34 [CH_3COOH]) and ion m/z 475 indicates loss of 18 Da (loss of the heterocyclic oxygen as H_2O). Lower intensity ions indicating a 2nd pathway of initial loss of 18 Da followed by 2 losses of 60 Da are also present (m/z 595, 535 and 475 respectively). There are also characteristic ions more directly indicative of the hopanoid nature of the compounds at m/z 191 as seen in the EI spectrum and at m/z 421 indicating neutral loss of the A+B rings from the protonated molecule. Low levels of a second, earlier eluting isomer (**1a'**; possibly the α,β isomer e.g. Eickhoff et al., 2014) were also present in some samples (Fig. 1a, Table 1).

In many samples, another peak (**1b**, Fig. 1a) was observed eluting just after anhydroBHT (**1a**) with a base peak ion of m/z 627, potentially indicating a methylated pseudohomologue of anhydroBHT. Based on the retention time this peak was anticipated to be the C-2 methylated homologue as the C-3 compound would elute later during both LCMS and GCMS analysis (e.g. Talbot et al., 2003; Farrimond et al., 2004), however, the expected m/z 205 ion (indicating methylation on the A+B rings) was not present (or only at very low relative abundance, see below) in the APCI MS² spectrum (Fig. 3d). An ion of m/z 191 was present suggesting instead an additional CH_2 located at a position other than on the A/B rings. Two ions indicating loss of 60 Da and one loss of 18 Da (m/z 567, 507 and 489

respectively; Fig. 3d) are also present in the spectrum of peak **Ib** (as also seen for anhydroBHT; Fig. 3b) as well as the ion indicative of neutral loss of 192 (m/z 435; Fig. 3d). We conclude, therefore, that this compound is related to anhydroBHT but has an additional methylation, possibly in the side chain. The D/E+side-chain fragment in the EI mass spectrum would therefore be an ion of m/z 405. Two peaks are observed in the EI m/z 405 mass chromatogram (Fig. 1b); one, (peak **Ib**) eluting directly after the main anhydroBHT isomer (**Ia**) and a 2nd peak eluting later (peak **IIIb**, Fig. 1b). The EI mass spectrum of peak **Ib** (Fig. 3c) is consistent with these interpretations, as it includes the ions indicative of a regular hopanoid not methylated on the A/B rings (m/z 191) or indeed any part of the ring system (m/z 369) as also seen for regular anhydroBHT, but also the expected M^+ and $[M-15]^+$ ions of m/z 626 and 611, respectively.

The second peak in the m/z 405 mass chromatogram (**IIIb**; Fig. 1b) was more difficult to characterise by EI mass spectrometry as it co-eluted with a number of other known compounds including BHT (peak **Ic**, Fig. 1b) and multiple isomers of 32,35-anhydrobacteriohopanepentol (anhydroPentol, **Id**; Fig 1b; Talbot et al., 2005). The retention time of the later eluting m/z 405 peak relative to peak **Ib** is suggestive of an additional methylation at the C-3 position (e.g. Farrimond et al., 2004), supported by the presence of the m/z 205 and 383 ions in the EI mass spectrum (Fig. 3e). This peak (**IIIb**) could also be observed in the APCI data as a peak in the m/z 641 ($= [M+H]^+$) mass chromatogram (Fig. 1a). The assignment of an A/B ring methylation is indicated by the ion m/z 205 in the MS² spectrum (Fig. 3f) and the neutral loss of 206 Da after loss of 2 acetylated hydroxyls to give m/z 315. The relative retention time of peaks **Ib** and **IIIb** by RP-HPLC (Fig. 1a) also agrees with previously reported separations between non-methylated and C-3 methylated homologues via RP-HPLC (regular C-2 methylated structure would elute between **Ib** and **IIIb**; e.g. Talbot et al., 2003b). Therefore peaks **Ib** and **IIIb** are proposed as a pair of novel compounds related to anhydroBHT but with an additional methylation in the side chain and differing from each other by the presence of a methyl group at C-3 in the latter compound.

354

355 In a few samples which contained peak **1b** ("side chain-methylated" anhydroBHT; see Table
356 1), a small shoulder was observed on the leading edge of this peak (peak **1a**, Fig. 1a). For
357 this shoulder, under APCI conditions, the MS² spectrum of *m/z* 627 did contain a small *m/z*
358 205 ion and it is therefore proposed to be the C-2 methylated homologue of anhydroBHT
359 (**1a**; e.g. Bednarczyk et al., 2005). However, this shoulder could not be readily distinguished
360 from the main, non-methylated compound and therefore measurements of peak **1b**
361 incorporate a minor contribution for peak **1a** which is estimated to account for less than 10%
362 of the main peak where present.

363

364 3.1.3 Novel N-containing BHPs

365 In addition to the "regular" N-containing biohopanoids (Figs. 2 and 4a-c) other N-containing
366 compounds were observed throughout the core including the recently described
367 "anhydroaminotriol" (**1i**, Figs. 2 and 4d; see Eickhoff et al., 2014). Identification of
368 anhydroaminotriol can be difficult by GCMS as the intensity of response of nitrogen
369 containing compounds via EI MS is much weaker than that of equivalent N-free compounds
370 (e.g. Eickhoff et al., 2014). Furthermore, under RP-HPLC-APCI-MS analysis,
371 anhydroaminotriol-triacetate co-elutes with regular aminotriol (peaks **1i** and **1f** respectively,
372 Fig. 2). In addition, the triacetate has a base peak ion of *m/z* 654 (= [M+H]⁺) which is
373 equivalent to the primary fragment ion of aminotriol under the same conditions (aminotriol
374 *m/z* 654 = [M+H-CH₃COOH]⁺; Fig. 4a; Talbot et al., 2003b,c). However, careful inspection of
375 the APCI data can still yield clues to the presence of this compound. Firstly, in the absence
376 of anhydroaminotriol, the intensity of the aminotriol base peak ion (MH⁺ = *m/z* 714) relative
377 to the *m/z* 654 ion (= [MH-CH₃COOH]⁺) in the full mass spectrum (Scan 1; Section 2.3) with
378 the conditions used is typically in the range 5:1. Therefore, when the observed ratio is closer
379 to 1:1 or higher as observed in several of the Cobham samples (Table 1, column *m/z*
380 654/*m/z* 714), it is clear that the transformation product is present. This assignment is also
381 supported by consideration of the MSⁿ spectra of *m/z* 714 and 654 respectively. It has

previously been shown that MS³ fragmentation of the *m/z* 654 ion derived from MS² of *m/z* 714 (aminotriol) leads to further fragmentation with ions *m/z* 594 and 534 as the major products (Talbot et al., 2003c). However, in the presence of anhydroaminotriol, during direct MS² fragmentation of *m/z* 654, the major ion observed is still *m/z* 654 (at 35% collision energy; Eickhoff et al., 2014), with lower intensity ions resulting from losses of 60 Da (acetylated OH groups at C-33 and C-34; Fig. 4d). This is a result of the stability of the heterocyclic N atom during ion-trap fragmentation. Anhydroaminotriol was present in most samples and was always the most abundant N-containing degradation product (Table 1). Adjustment of the anhydroaminotriol peak area for relative quantification is described in section 2.3.

We also identified 2 other compounds which we tentatively propose to be novel *N*-containing BHP transformation products. The MS² spectrum (Fig. 4e) of peak **Ik** from the APCI *m/z* 728 mass chromatogram (Fig. 2) indicates a N-containing compound (on the basis of the even numbered base peak ion) with a minor ion of *m/z* 191 (intensity typical of N-containing BHPs; e.g. Fig. 4c). The base peak ion is equivalent to that of regular A/B ring methylated-aminotriol (e.g. Talbot et al., 2008), however, if that were the case the peak should elute directly after aminotriol (peak **If**, Fig. 2; Talbot et al., 2003b; 2008). The peak in question actually elutes significantly earlier suggesting a more polar compound. Speculating therefore that the 14 Da difference could result from the incorporation of ketone oxygen into the molecule, it is reasonable to expect a loss of that oxygen atom as water (18 Da) under APCI conditions. The major fragment ion in the MS² spectrum is *m/z* 710 (base peak minus 18 Da; Fig. 4e) with 3 further losses of 60 Da (3 acetylated hydroxyls) and a minor ion at *m/z* 471 resulting from a final loss of an acetylated amine (see Fig. 4c for comparison of intensity of ion indicating loss of amine in aminopentol spectrum). It is therefore proposed that peak **Ik** (Fig. 2) is related to aminotriol and contains an amine, 3 hydroxyls and a ketone. Although the location of the ketone cannot be constrained other than excluding the A/B rings on the basis of the minor *m/z* 191 ion, there is one previous report of a highly functionalised BHP

containing a ketone oxygen at the C-32 position in the side chain. The composite structure 32-oxo-bacteriohopanetriol glucosamine (**Io**) was reported from *Zymomonas mobilis*, an obligately ethanologenic species of alphaproteobacteria (Flesch and Rohmer, 1989). It is therefore proposed that the most likely location for the ketone is at C-31 i.e. 31-oxo-35-amino-bacteriohopane-32,33,34-triol (31-oxo-aminotriol; Fig. 4e).

There was no equivalent peak in the m/z 786 chromatogram to indicate a possible hexafunctionalised compound (i.e. “30-oxo-aminotetrol”), even in the samples with the highest level of aminopentol. However, a peak of m/z 670 would correspond to the anticipated base peak for an aminodiol with additional ketone functionality. Peak **Ij**, the only significant peak in the m/z 670 mass chromatogram (Fig. 2), was considered to be a likely target. Note this retention time is too early to indicate a regular A/B ring methylated compound and the retention time relative to aminotriol (**If**) is early, as seen for the proposed ketone containing 31-oxo-amino-triol and aminotetrol (peaks **Ik** and **Ig** respectively, Fig. 2). Interpretation of this spectrum was complicated, however, as in many cases the peak co-eluted with an ion of m/z 669 meaning that the APCI spectrum contains fragments from both parent ions. Fragment ions of m/z 652, 610 and 550 were observed and would correspond exactly to the expected losses of the ketone oxygen as water or 2 acetylated OH functionalities. In this compound (**Ij**) the intensity of the $[M+H-18]^+$ ion (m/z 652) was significantly lower than for the equivalent ion (m/z 710) in the MS^2 spectrum of the proposed 31-oxo-aminotriol (**Ik**; Fig. 4e) whilst in the less functionalised compound, loss of the first acetylated hydroxyl (m/z 619) appears to be a more favourable fragmentation. A minor ion at 491 indicates loss of the acetylated OH groups and amine, prior to loss of the ketone, however, the hopanoid-specific ions at m/z 191 and 163 could be products of fragmentation of the co-eluting m/z 669 ion (see below). Therefore the assignment of peak **Ij** (Figs. 2 and 4f) as a tetrafunctionalised amine and ketone-containing BHP i.e. 32-oxo-35-amino-bacteriohopane-33,34-diol remains tentative but is included in further discussions below.

3.1.4 Other novel BHPs not containing a nitrogen atom

As mentioned above, a peak was observed in the m/z 669 APCI mass chromatogram which, in samples where co-elution with peak **lj** (m/z 670) was least significant, produced an APCI spectrum potentially indicating a polyfunctionalised BHP (Fig. 5a). Although a peak of m/z 669 would typically indicate an A/B ring methylated BHT (Talbot et al., 2003c) the early retention time (i.e. earlier than BHT; **lc**, Fig. 1a) indicates a more polar component. Assuming the validity of the assignment of peak **lk** (Figs. 2 and 4e) as a ketone-containing pentafunctionalised aminoBHP, it is then reasonable to assume that the same should be possible for BHPs which do not contain nitrogen i.e. structures related to BHT. A base peak of m/z 669 and retention time earlier than that of BHT is therefore suggestive of a BHT-ketone (m/z 669 = $[M+H-CH_3COOH]^+$). The APCI spectrum of peak **le** (Fig. 5a) shows three losses of 60 Da (m/z 609, 549 and 489 respectively) assumed to be the normal losses in the APCI spectrum of regular BHT (Talbot et al., 2003b,c). Although an ion of m/z 471 could be observed (loss of ketone oxygen as water from m/z 489), this was weak; nonetheless, the hopanoid nature of this peak is confirmed by the m/z 191, 163 and ions following neutral loss of the A+B rings (m/z 477, 417, 357; Fig. 5a).

As this compound does not contain N, an equivalent peak was sought in the GCMS data. The anticipated parent ion for this peracetylated compound would be m/z 728 under EI and, assuming a side chain location for the ketone, a D/E+side chain fragment 14 Da higher than that of BHT i.e. m/z 507 (relative to m/z 493, Fig 5b) is expected. A peak (m/z 507, **le**; Fig. 1b) was observed eluting after the main m/z 493 peak in the GCMS data (**lc**; Fig. 1b). The EI mass spectrum of peak **le** (Fig. 5b) contained the typical hopanoid fragments of m/z 191 and 369 excluding any further modification from the ring system. The predicted D/E-side chain fragment of m/z 507 was observed, however, so were two additional ions of m/z 447 and 387, potentially 2 losses of 60 Da from the full D/E-side chain fragment which are not typically observed in other EI spectra of functionalised BHPs (e.g. Fig. 3a) but may be due to the presence of the ketone. As the ring system ions restrict the location of the additional 14

Da to the side chain and in both the APCI and EI data, the relative retention time (compared to regular BHT; peak **1c**) indicates a more polar structure than that resulting from a simple methylation, we conclude that there is a ketone present in this structure, located somewhere in the side chain, most likely at C-31 i.e. 31-oxo-BHT (**1e**).

The tetrafunctionalised ketone equivalent (i.e. BHT with one OH replaced by ketone) would theoretically have an APCI base peak ion of m/z 611 ($[MH-CH_3COOH]^+$). Two peaks were observed in this mass chromatogram in many samples, however, they also co-elute exactly with peaks in the m/z 671 chromatogram (Fig. 1a). The latter ion is also previously reported as the base peak ion for anhydropentol (**1d**) which has a major fragment ion of m/z 611 (Fig. 5c; Talbot et al., 2005) so the tetrafunctionalised ketone could not be confirmed by APCI-MSⁿ. Under EI conditions, the D/E-side chain fragment of this proposed ketone would be m/z 449, identical to that of anhydropentol (Figs 1b; see Talbot et al., 2005) and therefore could not be confirmed due to co-elution with multiple BHPs (Fig. 5d) although the anticipated $[M-15]^+$ ion was present in low abundance (Fig. 5d). This compound is therefore excluded from the following discussion of relative abundance of the various known biohopanoids and novel BHPs including functionalised transformation products.

To summarise, a range of polyfunctionalised biohopanoids were identified including strong evidence for methanotroph-derived BHPs (aminotetrol and aminopentol in particular but also aminotriol) as well as a recently identified N-containing diagenetic product (anhydroaminotriol) and a number of putative novel diagenetic products including structures with an unusual side-chain methylation. A diverse range of ketone containing products, termed “oxo” BHPs on the basis of previous studies (Flesch and Rohmer, 1989), both with and without a nitrogen atom in the structure, are tentatively assigned here for the first time.

3.2 BHP variations in the Cobham Lignite sequence

The compounds BHT (**1c**), aminotriol (**1f**) and aminotetrol (**1g**) had very similar distributions in the sequence when converted to % total BHPs, with the highest relative abundance in the middle clay unit between the laminated and blocky lignite. However, these compounds were also relatively abundant in the uppermost laminated lignite and the lowest blocky lignite samples. Both of these lignite samples, to either side of the middle clay layer, also contained clay laminae not seen in any other lignite samples (Table 1). The combined total abundance of all biological BHPs relative to putative geo-BHPs shows two major and one minor peak (Fig. 6c). The first major peak begins in the uppermost laminated lignite and spans the middle clay layer reaching 100% biohopanoids at 65.3 cm (within the middle clay layer; Table 1). The second maximum of 76% occurs near the top of the Blocky Lignite at 118.65 cm (Table 1; note the blocky lignite continues above the section investigated here; Collinson et al., 2007; Steart et al., 2007). All biohopanoids show elevated levels in the samples from 115.65 and 118.65 cm except aminopentol which was only present in the lower of the two samples where it is at its highest relative abundance throughout the entire sequence (4%; Figs. 2 and 6, Table 1). The minor peak occurs in the single sand/mud unit sample underlying the Cobham Lignite sequence (Fig. 6c). At the onset of the CIE (Fig. 6a,b; 54-56 cm) relative abundances of BHT, aminotriol and aminopentol fluctuate markedly (Fig. 6d, e and g) whilst aminotetrol is consistently lower than in samples immediately pre and post this interval (Fig. 6f). Aminopentol (**1h**), however, was not present in the middle clay whilst both BHT and Aminotetrol had higher relative abundance (to total biohopanoids) in the middle clay layer and the adjacent lignite with clay samples (Table 1; Figs. 6d and 6f respectively).

The most abundant geo-BHP in the majority of samples was anhydroBHT (**1a**) accounting for up to 100% of all hopanoids (one sample; Fig. 7d, Table 1). Most of the geohopanoids followed a similar trend to anhydroBHT with high abundances relative to biohopanoids in lignites both above and below the middle clay layer (Table 1). This was particularly noticeable for the N-containing compounds in the laminated lignite, especially in samples leading up to and within the onset of the CIE just below the middle clay layer.

Anhydroaminotriol (**li**) reached a maximum of 45.8 % of the total BHPs and 50% of the total geohopanoids (40.65 cm, Table 1; Fig. 7g). The novel “side-chain methylated” anhydroBHTs (**lb** and **lllb**; Fig. 7e) and the proposed oxo-BHPs (**le**, **li**, **lj**; Fig. 7f, h-, Table 1) all had similar profiles through the sequence with peaks coinciding with the onset of the CIE and at the end or just after deposition of the middle clay layer.

4. Discussion

4.1 Origin of BHPs in the Cobham Lignite sequence

4.1.1 *Modern, Recent or Ancient deposition?*

Palaeoenvironmental interpretation of BHPs in the Cobham Lignite is contingent on these BHPs being formed in the ancient environment rather than being derived from bacteria living in the shallow subsurface at any point post deposition to date. Previous workers have shown that bacteria do live in subsurface environments including in marine sediments (e.g. Parkes et al., 2000; Kallmeyer et al., 2012), lignites and coalbeds (e.g. Kotelnikova, 2002; Pokorný et al., 2005). Inagaki et al. (2015) found unexpectedly high levels of microbial cells in lignite layers buried ~ 2 km below the ocean floor and microbial community analysis revealed populations similar to those found in forest soils. Aerobic organisms can receive low levels of oxygen via meteoric water in the subsurface environment (e.g. Kotelnikova, 2002) and specific aerobic methanotrophic activity was recently identified in Carboniferous coals where organisms affiliated with the Type I genera *Methylobacterium* and *Methylocaldum* and the Type II genera *Methylosinus* and *Methylocystis* were identified via 16S rRNA targeted gene sequencing after enrichment (Stepniewska et al., 2013). All of these genera have been shown to produce hopanoids (Cvejic et al., 2000; Talbot et al., 2001 and references therein; Banta et al., 2015), although both of the Type I genera identified are known to make both non-methylated and C-3 methylated biohopanoids (with a C-35 amine functionality), so are unlikely to be significant sources in the Cobham Lignite sequence which did not contain any

C-3 biohopanoids or hopanes (Pancost et al., 2007) and only one minor geohopanoid BHP (side chain-methylated-3-methylanhydroBHT, **IIIb**). In light of these findings it is difficult to preclude a modern origin for some of the biohopanoid BHPs at Cobham.

A modern origin for the Cobham Lignite BHPs, however, is considered unlikely for several reasons. Firstly, many aspects of the BHP distribution are consistent with an aerobic source which may be more recent but would also be consistent with formation in an ancient mire with abundant methanotrophs. Previously, carbon isotopic analysis of the hopanes in the same sample extracts (Fig. 6b, 7b; Pancost et al., 2007) supported a methanotrophic source. For example, within the upper part of the laminated lignite at the onset of the CIE, the $\delta^{13}\text{C}$ values of the C_{29} - and C_{31} $17\beta(H),21\beta(H)$ hopanes decrease (to values as low as -76‰ and -42‰, respectively), indicating the consumption of isotopically light methane (Pancost et al., 2007). This change in isotope values occurred within the laminated lignite (section 2.1; Fig. 6), but below the transitional zone to the middle clay where thin clay laminae start to appear in the lignite. Therefore the isotopic changes are not linked to changes in depositional environment (as far as those are expressed by changes in lithology) apparently precluding a preservation artefact (Pancost et al., 2007). Within the BHP assemblage, the co-occurrence of aminotriol (**If**) and aminotetrol (**Ig**) and with a **If/Ig** ratio less than 20 (as observed in all samples here, except that at 11.95 cm; Table 1) appears to be indicative of an aerobic methanotroph source. Indeed the value is more frequently below 10, whereas the lowest reported values for the only other known source of aminotetrol, anaerobic sulfate reducing bacteria of the genus *Desulfovibrio* (which are unlikely to occur in a freshwater environment) is over 20 and can be as high as 100 (Blumenberg et al., 2006, 2009, 2012; See also review in Talbot et al., 2014). An aerobic methanotroph source is also supported by the occurrence of aminopentol (**Ih**) in 13 samples covering all parts of the sequence, except the middle clay layer (and the lignite samples directly above and below the clay) where aminotetrol dominated (Figs. 6f and 8, Table 1).

Secondly, the strong increase in the relative proportion of biohopanoids in the middle clay layer and samples directly above and below containing clay laminae (Fig. 6c) is directly related to lithology. Low permeability of the clay layer compared to lignite would likely result in a much smaller “recent” population whilst the organic rich, more permeable lignite might be expected to host a larger “recent” population (cf. Inagaki et al., 2015). As the relative abundance of biohopanoid BHPs is in fact significantly lower in the lignite sections (Fig. 6c, 7c), this supports a sub-recent source for (some of) the BHPs with potentially better preservation of ancient BHPs in the fine grained material.

Thirdly, although modern bacteria could be affected by variations in lithology and organic matter content, they would not be expected to vary across the CIE onset, which occurs within the laminated lignite lithology below the transition zone to the clay layer (Figs. 6 and 7) where a distinct geohopanoid BHP signature with enhanced relative abundance of N-containing transformation products is observed (54.4 to 56.6 cm; Fig. 7h). Following the same argument made for the hopane isotope signature, that the lack of a change in lithology at this depth (54.4 to 56.6 cm) precludes a preservation artefact (Pancost et al., 2007), then an alternative explanation is required to explain the relative increase in ketone-containing compounds (Fig. 7f,h). As the pathway for production of the proposed ketone-containing compounds is currently unknown, they may represent either a specific transformation pathway, or could be derived from as yet unknown biological sources. The only previous report of a ketone containing biohopanoid was from the obligately ethanologenic bacterium *Zymomonas mobilis* (alphaproteobacteria; Flesch and Rohmer, 1989). This organism was cultured under microaerophilic conditions and the authors proposed that the compound 32-oxo-BHT glucosamine (**1o**) could be either a precursor or catabolite of BHT (Flesch and Rohmer, 1989). Gibson (2011) also tentatively identified ketone-containing polyfunctionalised hopanoids (without nitrogen) in geothermal sinters that were precipitating under microaerophilic conditions. We therefore tentatively propose that the oxo-amineBHPs could represent production by methanotrophs under oxygen limited conditions.

604

605 Finally, no composite BHPs (structures containing a more complex moiety at the C-35
606 position such as an aminosugar; e.g. **Im**, **In**; Rohmer, 1993) were observed, even in the clay
607 layer, although these compounds would be expected in any modern or Recent terrestrial
608 setting (e.g. Cooke et al., 2008a; van Winden et al., 2012a,b; Spencer Jones et al., 2015)
609 including marine sediments containing high terrestrial fluvial input (e.g. Handley et al., 2010;
610 Wagner et al., 2014). Furthermore, adenosylhopane (**Ip**), and compounds related to this
611 structure containing an alternative terminal moiety at C-35 with or without A-ring methylation
612 (**I** or **Ilq**) (e.g. Cooke et al., 2008a; Rethemeyer et al., 2010), were also absent from the
613 Cobham sequence, despite being nearly ubiquitous in terrestrial settings (see review in
614 Spencer-Jones et al., 2015). This is not surprising, if the BHPs that are present are indeed of
615 Eocene age, as adenosylhopane was found to be degraded more rapidly than all other
616 functionalised BHPs, including aminoBHPs, in a study of sediments up to 1.2 Ma from the
617 Congo deep-sea fan (ODP site 1075; Cook et al., 2008b; Handley et al., 2010).
618 Adenosylhopane was also completely removed/transformed during an artificial maturation
619 experiment on biomass of the purple non-sulfur bacterium *Rhodopseudomonas palustris*,
620 whilst some BHT (**lc**) and aminotriol (**lf**) remained after exposure to elevated pressure and
621 temperature (170°C, 120 MPa, 7 d; Eickhoff et al., 2014).

622

623 Collectively, this evidence suggests that at least some of the BHPs, and the oxo-compounds
624 in particular (Fig. 7f,h), could reflect environmental conditions associated with the original
625 deposition of the lignite. Nonetheless, a more recent source can neither be confirmed nor
626 entirely excluded and we suggest that future work conduct BHP analyses in tandem with
627 microbiological investigations (i.e. cell counts, enrichments) in an attempt to decouple
628 ancient from modern living bacterial contributions. If, however, the biohopanoid BHPs in the
629 Cobham lignite are indeed of the same age as the deposition of the lignite, this would
630 represent the oldest example of suites of solvent extractable intact biohopanoids reported to
631 date. Previously only BHT has been identified in TLE from Tanzanian sediments up 50 Ma

(van Dongen et al., 2006) and following chemical degradation of the Messel oil shale kerogen (Eocene, 50 Ma; Mycke et al., 1987). If contemporaneous with lignite deposition then this significantly extends the aminoBHP record back in time, by nearly 55 Ma, highlighting their potential utility in identifying the aerobic methane oxidation process in samples where other methods can be inconclusive.

4.1.2 Variability in methanotrophic sources

The occurrence of aminopentol (**lh**), thought to be a marker for Type I methanotrophs in terrestrial settings (see review in Talbot et al., 2014), in 13 Cobham Lignite samples is consistent with a significant methanotroph input. In recent studies aminopentol accounted for only a very minor proportion of the full biohopanoid BHP complement in a range of European *Sphagnum* peat sections (<1%; van Winden et al., 2012a,b; Talbot and Pancost, unpublished data). In contrast, the highest abundance of aminopentol relative to total biohopanoid BHPs in the Cobham Lignite reaches ~20% (sample 115.65 cm; Fig. 6g) or 4% relative to total BHPs (Table 1), significantly higher than that observed in any *Sphagnum* sample or modern peat. Furthermore, the peak occurrence of aminopentol (115.65 cm, Fig. 6g) corresponds to a C₂₉ hopane carbon isotope ratio of -53.2‰ which, although less than the maximum depletion during the onset of the CIE, is still significantly depleted relative to pre-CIE values in the lower Laminated lignite (range -40.5 to -31.0‰; Fig 6b). Also, 3 of the 5 samples at the onset of the CIE where C₂₉ carbon isotope ratio reach values as low as -75.7‰ also contain relatively high levels of aminopentol (up to 10% of total biohopanoids, Fig. 6g). The sample at 70.3 cm, slightly above the clay layer also contains similar levels of aminopentol and again corresponds to strongly depleted signature for the C₂₉ hopane of -61.77‰ (Fig. 6b). Clearly there is correspondence in the Cobham Lignite between aminopentol abundances (as proportions of total biohopanoids) and ¹³C-depleted isotopic composition of the C₂₉ hopane. Moreover, maxima in aminopentol proportions and minima in C₂₉ hopane δ¹³C values also correspond to maxima in abundances of nitrogen and ketone-containing degradation products (Fig. 7h).

Aminotetrol (**Ig**) is also likely derived from methanotrophs in this terrestrial setting. It has also been found only at very low levels in *Sphagnum* peat (<2% of total BHPs) such that its relative abundance in the Cobham Lignite, reaching a maximum of ~65% of total biohopanoid BHPs (Fig. 6f, 4.65 cm; equivalent to 14.4% of total BHPs; Table 1) is remarkable, likely reflecting intense methanotrophic activity. Intriguingly and in contrast to aminopentol, aminotetrol proportions do not appear to track hopane $\delta^{13}\text{C}$ values; in part, that could reflect changing methanotroph communities as discussed below.

Aminotriol (**If**) and BHT (**Ic**) are much more significant components in peat (van Winden et al., 2012a,b; Talbot and Pancost, unpublished data) than aminopentol and aminotetrol. They are present throughout the Cobham sequence likely indicating a combination of sources including Type II methanotrophs and heterotrophs (e.g. van Winden et al., 2012a). Again, variations in their proportions do not correspond to those of hopane $\delta^{13}\text{C}$ values, suggesting that they either do not derive from methanotrophs or derive from a different group of methanotrophs, exhibiting different behaviour.

The BHP composition of both the lower laminated lignite (deposited during the latest Palaeocene) and upper blocky lignite (deposited during the PETM) are broadly similar (Fig. 8a,d), suggesting the microbiological community was similar during both periods of deposition or during later colonisation. If the former, this is unexpected given the wetter conditions and presumably greater methane cycling (as inferred from hopane $\delta^{13}\text{C}$ values) in the upper section, although Sherry et al. (2016) showed that there was no significant changes in the overall methanotrophic community distribution in sediment slurry incubations under a range of methane concentrations. Nonetheless, the blocky lignite is associated with generally higher proportions of aminopentol (Fig. 6g) and that does suggest that aspects of the biohopanoids BHP distribution are recording environmental change.

687

688 The most significant change in biohopanoid BHPs, both in terms of their abundance relative
689 to total BHPs and their distribution, occurs in the clay layer (and lignite with clay; Fig. 8c,
690 Table 1). Biohopanoid BHPs represented the highest proportion of total BHPs in the clay
691 layer, up to 100% at 65.3 cm (Fig. 6c; Table 1), which we attribute to enhanced preservation
692 (see above, section 4.1.1). With respect to the biohopanoid BHP distribution, the most
693 striking feature in the clay layer is the absence of aminopentol (**lh**), particularly given the
694 high abundances of both aminotriol (**lf**) and aminotetrol (**lg**; Figs. 6e and f, 8b, Table 1). This
695 could reflect a change in the depositional environment: the clay layer has been linked to
696 changes in local hydrology leading to increased run-off and even standing water as indicated
697 by the occurrence of *Salvinia* and *Azolla* (free floating water plants) at the base of the blocky
698 lignite directly above the clay, possibly facilitated by deposition of clay reducing drainage
699 (Collinson et al., 2003, 2013; Steart et al., 2007 and references therein). This could have
700 impacted bacterial or even methanotroph communities and associated BHP signatures.

701

702 The presence of aminotetrol and absence of aminopentol has been linked to Type II
703 methanotroph sources (e.g. Talbot et al., 2001; Birgel et al., 2011), although some Type I
704 methanotrophs also do not produce aminopentol (Talbot et al., 2001; Jahnke et al., 1995;
705 Coolen et al., 2008; Banta et al., 2015). Nonetheless, it is possible that the different
706 distributions in the clay layer reflect different environmental conditions and a methanotroph
707 community dominated by Type II organisms. These are traditionally believed to be common
708 in terrestrial settings (soils, peats e.g. Hanson and Hanson, 1996), although this is certainly
709 not always the case. For example, Gray et al. (2014) found that Type I methanotrophs
710 dominated over Type II signals in soil cores from 13 sites located along the southern and
711 northern margins of Kongsfjorden in Northwestern Spitsbergen. Overall, it remains unclear
712 what dictates the predominance of different types of methanotrophs, and therefore, it is
713 difficult to explain a change in assemblages in the Cobham Lignite.

4.2 Known and novel polyfunctionalised hopanoid transformation products in the Cobham

Lignite sequence

4.2.1. AnhydroBHT and related structures

The most abundant degradation product, occurring in all but one sample (65.3 cm; Table 1) in the Cobham sequence was anhydroBHT (**la**). This is expected as the compound has been shown to be produced from BHT (**lc**) and composite structures such as BHT cyclitol ether (**lm**) under a range of conditions (Schaeffer et al., 2008, 2010; Eickhoff et al., 2014). It has been reported in a wide range of samples as old as Jurassic in age (Bednarczyk et al., 2005) and was by far the most abundant BHP in a ~50 Ma marine sediment sample from Tanzania (van Dongen et al., 2006). Watson (2002), also showed a correlation between loss of BHT and increase in anhydroBHT in sediments from the Benguela upwelling system down to over 4 Ma, as did Blumenberg et al. (2013) in younger sediments from the Baltic Sea. Whilst it is yet to be conclusively demonstrated that adenosylhopane (**lp**; or related compounds, **lq**) could also be a precursor for this transformation product, a number of studies have speculated that it may be possible via reductive removal of the terminal adenine (Costantino et al., 2001; Cooke et al., 2008b; Eickhoff et al., 2014). The high abundance of anhydroBHT in these samples, therefore, likely indicates an amalgamated signature from a range of precursor biohopanoids.

By careful inspection of the APCI and EI data we have identified 2 novel structures related to anhydroBHT (**la**) but containing an unusual methylation in the side chain (Figs. 1 and 3). The location of the unusual side chain methylation could not be conclusively determined based on the available data and insufficient material is available to attempt isolation and NMR analysis. Previously, however, Simonin et al. (1994) identified biohopanoids with methylation at the C-31 position of the side chain of hopanoids from the acetic acid bacterium *Acetobacter europaeus* (Phylum Alphaproteobacteria, also known as *Gluconacetobacter europaeus* or *Komagataeibacter europaeus*). The side chain methylated compounds in that study were also methylated at the C-3 position as in compound **IIlb** reported here (Fig. 3).

More recently, Nytoft (2011) reported C-31 methylated hopanes, although not additionally methylated at the C-3 position, in coals and crude oils sourced from a range of locations worldwide and linked these compounds with oxic depositional environments. The possible occurrence of C-3 methylation in one of these structures (**IIIb**), the only proposed C-3 methylated compound in the entire data set, does agree with the potential acetic acid bacterium source (Simonin et al., 1994); therefore the tentative structures are illustrated with the methylation at C-31 (**Ib** and **IIIb**; Fig. 3 and Appendix). An alternative known site for methylation at C-12 as reported for a BHT in the sponge *Placortis simplex* (Costantino et al., 2000) could be conclusively ruled out for structure **Ib** due to the presence of the m/z 369 ion in the EI spectrum (Figs. 3c). No C-3 methylated precursor biohopanoids were observed in the Cobham sequence; however, given the low relative intensity of peak **IIIb** (Fig. 1; Table 1), this is not surprising, especially when considering that reports of other C-3 methylated biohopanoids in younger samples are scarce (e.g. Talbot et al., 2003a; Talbot and Farrimond, 2007; Blumenberg et al., 2007; Gibson et al., 2008; Zhu et al., 2011).

We are not aware of prior reports of polyfunctionalised biohopanoids with this unusual side-chain methylation in environmental samples. The relative retention time of **Ib** to anhydroBHT (**Ia**; Fig. 1) indicates that it would elute in approximately the same position as the regular C-2 methylated homologue (**IIa**; Fig.1). However, in various settings an apparently methylated BHT eluting at the expected C-2 methyl position (i.e. directly after BHT by RP-HPLC) has been observed in sediment extracts but where the MS² spectrum contains a dominant m/z 191 and only a minor m/z 205 ion (if present at all; Talbot et al., unpublished data).

There was no evidence of C-2 methylated biohopanoid precursors in any of the samples, and only trace levels of a C-2 methylated anhydroBHT (**IIa**) could be identified in a few samples indicating that some C-2 methylated precursor was occasionally present. Absence of C-2 methylated structures is relatively unusual for terrestrial settings, as they are frequently found, for example, in soils (e.g. Cooke et al., 2008a; Xu et al., 2009; Rethemeyer

et al., 2010; Kim et al., 2011; Zhu et al., 2011), lake sediments (Talbot et al., 2003a; Talbot and Farrimond, 2007; Coolen et al., 2008) and tropical wetlands (Wagner et al., 2014; Spencer-Jones et al., 2015). As the co-eluting peak **lb** was in all cases significantly more intense than the shoulder **lla** (e.g. Fig. 1a), the compounds could not be individually integrated and are combined in Table 1. Furthermore, peak **lla** could not be conclusively identified by GCMS analysis.

4.2.2 *N*-containing transformation products.

Crucially, this study has revealed the presence of both previously identified and novel transformation products of N-containing BHPs, providing new tools for examining methane cycling in ancient settings. These observations are consistent with recent experimental work. Eickhoff et al. (2014) reported the generation of a pair of novel *N*-containing transformation products during simulated diagenetic degradation of a culture of the purple non-sulfur bacterium *Rhodopseudomonas palustris*. These structures, tentatively identified as isomers of anhydroaminotriol (**li**; Fig. 4d), were major components of the products after artificial maturation. Their finding is significant as it represents the first polyfunctionalised N-containing hopanoid degradation product indicating a possible distinct transformation pathway for hopanoids containing a terminal amine (Eickhoff et al., 2014). The observation of the later eluting and therefore presumed $\beta\beta$ isomer here in the Cobham Lignite represents the first report of this compound from environmental samples. Moreover, other N-containing products are tentatively proposed here (oxo-aminotriol [**lk**] and oxo-aminodiol [**lj**]; Figs 2 and 4, Table 1). Anhydroaminotriol was by far the most abundant compound of this type during the onset of the CIE (Fig. 8c; Table 1), although its peak occurrence was in the sample from 40.65 cm suggesting that nitrogen containing precursors were particularly abundant at the time of deposition of this sample. However, bulk and compound specific isotope values do not indicate an enhancement in methane cycling at this point (Fig. 7; Pancost et al., 2007) and therefore suggest heterotrophic sources for the precursor aminotriol.

5. Conclusions

This study presents the first identification of polyfunctionalised bio- and geohopanoids in the well preserved, immature Cobham Lignite sequence from within part of the PETM interval (~56 Ma) and below. Up to four different biohopanoids including BHT, aminotriol, aminotetrol and aminopentol were observed in samples throughout the sequence. Although the age of the BHPs cannot be constrained at this time, several lines of evidence point to a sub-Recent, predominantly methanotrophic source for the BHPs. These include prior reports of isotopically light hopanes (up to -74‰) indicative of enhanced methanotrophy at the onset of the negative CIE, the absence of the composite biohopanoids or adenosylhopane and related structures, and peaks in novel, potentially ketone containing, geohopanoid BHP transformation products corresponding to the onset of the CIE.

The comparable averaged BHP distribution in the lower laminated lignite (deposited during the latest Paleocene) and the blocky lignite (deposited during the PETM) suggest similar dominant members of the microbiological community were active during both periods. This is unexpected given the wetter conditions and the presence of generally more ¹³C-depleted hopanes in the blocky lignite although there are subtle differences in the intermittent occurrence of aminopentol which corresponds with depleted C₂₉ hopane δ¹³C values.

Further experimental work (e.g. quantitative BHP analysis; laboratory studies of the impact of different environmental conditions [temperature, methane concentration etc.] on BHP distributions) and study of other lignites including cell counts, formed under both changing and constant climatic conditions, is needed to interpret the palaeoenvironmental implications of the methanotroph communities and their varied biomarkers.

ACKNOWLEDGEMENTS

We thank Alfred McAlpine plc, AMEC and Channel Tunnel Rail Link for access to the Cobham Lignite sequence, and S. Rose for making arrangements; J. Hooker, J. Skipper and S. Tracey for help with sample collection and field discussions. We thank J. Hooker for his contributions to the understanding of the stratigraphy of the site. We acknowledge funding support for this research from the Leverhulme Trust (Grant number F/07/537/0) and the Natural Environment Research Council [Grant numbers NE/J008656/1] [NE/J008591/1]. This project was also partially funded by a Starting Grant (No. 258734) awarded to HMT for project AMOPROX from the European Research Council (ERC) and we also thank the Natural Environment Research Council (NERC) for funding JB (Grant number NE/I027967/1). We also thank the Science Research Investment Fund (SRIF) from HEFCE for funding the purchase of the ThermoFinnigan LCQ ion trap mass spectrometer (Newcastle) and Paul Donohoe, Kate Osborne, Luke Handley, Frances Sidgwick and David Steart for technical assistance. Finally, we thank the associate editor and reviewers Martin Blumenberg and Alex Sessions for their critical reviews which helped to significantly improve the manuscript.

References

- Banta, A., Wei, J.H., Welander, P.V., 2015. A distinct pathway for tetrahymanol synthesis in bacteria. *Proceedings of the National Academy of Science of the USA* 112, 13478-13483.
- Bednarczyk, A., Hernandez, T.C., Schaeffer, P., Adam, P., Talbot, H.M., Farrimond, P., Riboulleau, A., Largeau, C., Derenne, S., Rohmer, M., Albrecht, P., 2005. 32,35-Anhydrobacteriohopanetetrol: An unusual bacteriohopanepolyol widespread in recent and past environments. *Organic Geochemistry* 36, 673–677.
- Berndmeyer, C., Thiel, V., Schmale, O., Blumenberg, M., 2013. Biomarkers for aerobic methanotrophy in the water column of the stratified Gotland Deep (Baltic Sea). *Organic Geochemistry* 55, 103-111.
- Birgel, D., Feng, D., Roberts, H.H., Peckmann, J., 2011. Changing redox conditions at cold seeps as revealed by authigenic carbonates from Alaminos Canyon, northern Gulf of Mexico. *Chemical Geology* 285, 82–96.
- Blumenberg, M., Krüger, M., Nauhaus, K., Talbot, H.M., Oppermann, B.I., Seifert, R., Pape, T., Michaelis, W., 2006. Biosynthesis of hopanoids by sulfate-reducing bacteria (genus *Desulfovibrio*). *Environmental Microbiology* 8, 1220–1227.
- Blumenberg, M., Seifert, R., Michaelis, W., 2007. Aerobic methanotrophy in the oxic–anoxic transition zone of the Black Sea water column. *Organic Geochemistry* 38, 84–91.
- Blumenberg, M., Oppermann, B.I., Guyoneaud, R., Michaelis, W., 2009. Hopanoid production by *Desulfovibrio bastinii* isolated from oilfield formation water. *FEMS Microbiology Letters* 293, 73–78.
- Blumenberg, M., Mollenhauer, G., Zabel, M., Reimer, A., Thiel, V., 2010. Decoupling of bio and geohopanooids in sediments of the Benguela Upwelling System (BUS). *Organic Geochemistry* 41, 1119–1129.
- Blumenberg, M., Hoppert, M., Krüger, M., Dreier, A., Thiel, V., 2012. Novel findings on hopanoid occurrences among sulfate reducing bacteria: is there a direct link to nitrogen fixation? *Organic Geochemistry* 49, 1–5.

867 Blumenberg, M., Berndmeyer, C., Moros, M., Muschalla, M., Schmale, O., Thiel, V., 2013.
 868 Bacteriohopanepolyols record stratification, nitrogen fixation and other biogeochemical
 869 perturbations in Holocene sediments of the Central Baltic Sea. *Biogeosciences* 10, 2725-
 870 2735.

871 Bodlenner, A., Liu, W.H., Hirsch, G., Schaeffer, P., Blumenberg, M., Lendt, R., Tritsch, D.,
 872 Michaelis, W., Rohmer, M., 2015. C35 Hopanoid Side Chain Biosynthesis: Reduction of
 873 Ribosylhopane into Bacteriohopanetetrol by a Cell-Free System from *Methylobacterium*
 874 *organophilum*. *ChemBioChem* 16, 1764-1770.

875 Bradley, A.S., Pearson, A., Saenz, J.P., Marx, C.J., 2010. Adenosylhopane: The first
 876 intermediate in hopanoid side chain biosynthesis. *Organic Geochemistry* 41, 1075-1081.

877 Burhan, R.Y.P., Trendel, J.M., Adam, P., Wehrung, P., Albrecht, P., Nissenbaum, A. 2002.
 878 Fossil bacterial ecosystem at methane seeps: origin of organic matter from Be'eri sulphur
 879 deposit, Israel. *Geochimica et Cosmochimica Acta* 66, 4085–4101.

880 Collinson, M.E., Hooker, J.J., Gröcke, D.R., 2003. Cobham Lignite Bed and
 881 penecontemporaneous macrofloras of southern England: A record of vegetation and fire
 882 across the Paleocene-Eocene Thermal Maximum. *Geological Society of America Special*
 883 *Papers* 369, 333-349.

884 Collinson, M.E., Steart, D.C., Scott, A.C., Glasspool, I.J., Hooker, J.J., 2007. Episodic fire,
 885 runoff and deposition at the Palaeocene-Eocene boundary. *Journal of the Geological*
 886 *Society, London* 164, 87-97.

887 Collinson, M.E., Steart, D.C., Harrington, G.J., Hooker, J.J., Scott, A.C., Allen, L.O.,
 888 Glasspool, I.J., Gibbons, S.J., 2009. Palynological evidence of vegetation dynamics in
 889 response to palaeoenvironmental change across the onset of the Paleocene-Eocene
 890 Thermal maximum at Cobham, Southern England. *Grana* 48, 38-66.

891 Collinson, M.E., Smith, S.Y., van Konijnenburg-van Cittert, J.H.A., Batten, D.J., van der
 892 Burgh, J., Barke, J., Marone, F., 2013. New observations and synthesis of Paleogene
 893 heterosporous water ferns. *International Journal of Plant Sciences* 174, 350-363.

894 Collister, J.W., Summons, R.E., Lichtfouse, E., Hayes, J.M., 1992. An isotopic
 895 biogeochemical study of the Green River oil shale. *Organic Geochemistry* 19, 265–276.

896 Cooke, M.P., Talbot, H.M., Farrimond, P., 2008a. Bacterial populations recorded in
 897 bacteriohopanepolyol distributions in soils from Northern England. *Organic Geochemistry*
 898 39, 1347–1358.

899 Cooke, M.P., Talbot, H.M., Wagner, T., 2008b. Tracking soil organic carbon transport to
 900 continental margin sediments using soil-specific hopanoid biomarkers: a case study from
 901 the Congo fan (ODP site 1075). *Organic Geochemistry* 39, 965–971.

902 Coolen, M.J.L., Talbot, H.M., Abbas, B.A., Ward, C., Schouten, S., Volkman, J.K., Sinninghe
 903 Damsté, J.S., 2008. Sources for sedimentary bacteriohopanepolyols as revealed by 16S
 904 rDNA stratigraphy. *Environmental Microbiology* 10, 1783-1803.

905 Costantino, V., Fattorusso, E., Imperatore, C., Mangoni, A., 2000. The First 12-
 906 Methylhopanoid: 12-Methylbacteriohopanetetrol from the Marine Sponge *Plakortis*
 907 *simplex*. *Tetrahedron* 56, 3781-3784.

908 Costantino, V., Fattorusso, E., Imperatore, C., Mangoni, A., 2001. A biosynthetically
 909 significant new bacteriohopanoid present in large amounts in the Caribbean sponge
 910 *Plakortis simplex*. *Tetrahedron* 57, 4045–4048.

911 Cvejic, J.H., Bodrossy, L., Kovacs, K.L., Rohmer, M., 2000. Bacterial triterpenoids of the
 912 hopane series from the methanotrophic bacteria *Methylocaldum* spp.: phylogenetic
 913 implications and first evidence for an unsaturated aminobacteriohopanepolyol. *FEMS*
 914 *Microbiology Letters* 182, 361–365.

915 Eickhoff, M., Birgel, D., Talbot, H.M., Peckmann, J., Kappler, A., 2014. Early diagenetic
 916 degradation products of bacteriohopanepolyols produced by *Rhodopseudomonas*
 917 *palustris* strain TIE-1. *Organic Geochemistry* 68, 31–38.

918 Farrimond, P., Talbot, H.M., Watson, D.F., Schulz, L.K., Wilhelms, A., 2004.
 919 Methylhopanoids: Molecular indicators of ancient bacteria and a petroleum correlation
 920 tool. *Geochimica et Cosmochimica Acta* 68, 3873-3882.

921 Flesch, G., Rohmer, M., 1989. Prokaryotic triterpenoids. A novel hopanoid from the ethanol-
 922 producing bacterium *Zymomonas mobilis*. Biochemical Journal 262, 673-675.

923 Gibson, R.A., 2011. The distribution of bacteriohopanepolyols in terrestrial geothermal
 924 ecosystems. PhD Thesis, Newcastle University, UK.
 925 <https://theses.ncl.ac.uk/dspace/bitstream/10443/1104/1/Gibson11.pdf>

926 Gibson R.A., Kaur, P., Pancost, R.D., Mountain, B., Talbot, H.M., 2008.
 927 Bacteriohopanepolyol signatures of cyanobacterial and methanotrophic bacterial
 928 populations recorded in a geothermal vent sinter. Organic Geochemistry 39, 1020-1023.

929 Gibson, R.A., Sherry, A., Kaur, G., Pancost, R.D., Talbot, H.M., 2014.
 930 Bacteriohopanepolyols preserved in silica sinters from Champagne Pool (New Zealand)
 931 record the environmental history of the vent. Organic Geochemistry 69, 61–69.

932 Gray, N.D., McCann, C.M., Christgen, B., Ahammad, S.Z., Roberts, J.A., Graham, D.W.,
 933 2014. Soil geochemistry confines microbial abundances across an Arctic landscape;
 934 Implications for net carbon exchange with the atmosphere. Biogeochemistry 120, 307-
 935 317.

936 Handley, L., Talbot, H.M., Cooke, M.P., Anderson, K.E., Wagner, T., 2010.
 937 Bacteriohopanepolyols as tracers for continental and marine organic matter supply and
 938 phases of enhanced nitrogen cycling on the late Quaternary Congo deep sea fan.
 939 Organic Geochemistry 41, 910–914.

940 Hanson, R.H., Hanson, T.E., 1996. Methanotrophic bacteria. Microbiological Reviews 439–
 941 471.

942 Inagaki, F., Hinrichs, K.-U., Kubo, Y., Bowles, M.W., Heuer, V.B., Hong, W.-L., Hoshino, T.,
 943 Ijiri, A., Imachi, H., Ito, M., Kaneko, M., Lever, M.A., Lin, Y.-S., Methé, B.A., Morita, S.,
 944 Morono, Y., Tanikawa, W., Bihan, M., Bowden, S.A., Elvert, M., Glombitza, C., Gross, D.,
 945 Harrington, G.J., Hori, T., Li, K., Limmer, D., Liu, C.-H., Murayama, M., Ohkouchi, N.,
 946 Ono, S., Park, Y.-S., Phillips, S.C., Prieto-Mollar, X., Purkey, M., Riedinger, N., Sanada,
 947 Y., Sauvage, J., Snyder, G., Susilawati, R., Takano, Y., Tasumi, E., Terada, T., Tomaru,

948 H., Trembath-Reichert, E., Wang, D.T., Yamada, Y., 2015. Exploring deep microbial life in
 949 coal-bearing sediment down to ~2.5 km below the ocean floor. *Science* 349, 420-424.

950 Jahnke, L.L., Summons, R.E., Dowling, L.M., Zahiralis, A.D., 1995. Identification of
 951 methanotrophic lipid biomarkers in cold-seep mussel gills: chemical and isotopic analysis.
 952 *Applied and Environmental Microbiology* 61, 576–582.

953 Jahnke, L.L., Summons, R.E., Hope, J.M., Des Marais, D.J., 1999. Carbon isotopic
 954 fractionation in lipids from methanotrophic bacteria II: the effects of physiology and
 955 environmental parameters on the biosynthesis and isotopic signatures of biomarkers.
 956 *Geochimica et Cosmochimica Acta* 63, 79–93.

957 Kallmeyer, J., Pockalny, R., Adhikari, R.R., Smith, D.C., D'Hondt, S., 2012. Global
 958 distribution of microbial abundance and biomass in subseafloor sediment. *Proceedings of*
 959 *the National Academy of Sciences* 109, 16213-16216.

960 Kannenberg, E.L., Poralla, K., 1999. Hopanoid biosynthesis and function.
 961 *Naturwissenschaften* 86, 168–176.

962 Kim, J.-J., Talbot, H.M., Zarzycka, B., Bauersach, T., Wagner, T., 2011. Occurrence and
 963 abundance of soil-specific bacterial membrane lipid markers in the Têt watershed
 964 (Southern France): soil-specific BHPs and branched GDGTs. *Geochemistry, Geophysics,*
 965 *Geosystems* 12, number 2. doi:10.1029/2010GC003364

966 Kotelnikova, S., 2002. Microbial production and oxidation of methane in deep subsurface.
 967 *Earth-Science Reviews* 58, 367 – 395.

968 Kulkarni, G., Wu, C.-H., Newman, D.K., 2013. The general stress response factor EcfG
 969 regulates expression of the C-2 hopanoid methylase *HpnP* in *Rhodopseudomonas*
 970 *palustris*TIE-1. *Journal of Bacteriology* 195, 2490-2498.

971 Liu, W., Sakr, E., Schaeffer, P., Talbot, H.M., Kannenberg, E., Donisi, J., Poralla, K.,
 972 Takano, E., Rohmer, M., 2014. Ribosylhopane, a novel bacterial hopanoid, as precursor
 973 of C35 bacteriohopanepolyols in *Streptomyces coelicolor* A3(2). *ChemBiochem.* 15,
 974 2156-2161.

975 McInerney, F.A., Wing. S.L., 2011. The Paleocene-Eocene Thermal Maximum: A
 976 Perturbation of Carbon Cycle, Climate, and Biosphere with Implications for the Future.
 977 Annual Review of Earth and Planetary Sciences 39, 489–516.

978 Mycke, B., Narjes, F., Michaelis, W., 1987. Bacteriohopanetetrol from chemical degradation
 979 of an oil shale kerogen. Nature 326, 179 – 181.

980 Neunlist, S., Rohmer, M., 1985. Novel hopanoids from the methylotrophic bacteria
 981 *Methylococcus capsulatus* and *Methylomonas methanica* - (22S)-35-
 982 Aminobacteriohopane-30,31,32,33,34-pentol and (22S)-35-amino-3- β -
 983 methylbacteriohopane-30,31,32,33,34-pentol. Biochemical Journal 231, 635-639.

984 Nytoft, H.P., 2011. Novel side chain methylated and hexacyclic hopanes: Identification by
 985 synthesis, distribution in a worldwide set of coals and crude oils and use as markers for
 986 oxic depositional environments. Organic Geochemistry 42, 520-539.

987 Ourisson, G., Albrecht, P., 1992. Hopanoids. 1. Geohopanoids: The most abundant natural
 988 products on Earth? Accounts of Chemical Research 25, 398–402.

989 Ourisson, G., Rohmer, M., Poralla, K., 1987. Prokaryotic hopanoids and other polyterpenoid
 990 sterol surrogates. Annual Review of Microbiology. 41, 301–333.

991 Pancost, R.D., Steart, D.S., Handley, L., Collinson, M.E., Hooker, J.J., Scott, A.C.,
 992 Grassineau, N.V., Glasspool, I.J., 2007. Increased terrestrial methane cycling at the
 993 Palaeocene-Eocene thermal maximum. Nature 449, 332-335.

994 Parkes, R.J., Cragg, B.A., Wellsbury P., 2000. Recent studies on bacterial populations and
 995 processes in subseafloor sediments: A review. Hydrogeology Journal 8, 11–28.

996 Pearson, A., Page, S.R.F., Jorgenson, T.L., Fischer, W.W., Higgins, M.B., 2007. Novel
 997 hopanoid cyclases from the environment. Environmental Microbiology 9, 2175-2188.

998 Pearson, A., Leavitt, W.D., Sáenz, J.P., Summons, R.E., Tam, M.C.M., Close, H.G., 2009.
 999 Diversity of hopanoids and squalene-hopene cyclases across a tropical land-sea
 1000 gradient. Environmental Microbiology 11, 1208-1223.

1001 Pokorný, R., Olejníková, P., Balog, M., Zifčák, Hölker, U., Janssen, M., Bend, J., Höfer, M.,
 1002 Holienčin, R., Hudecová, D., Varečka, L., 2005. Characterization of microorganisms

1003 isolated from lignite excavated from the Záhorie coal mine (southwestern Slovakia).
 1004 Research in Microbiology 156, 932–943.
 1005 Rethemeyer, J., Schubotz, F., Talbot, H.M., Cooke, M.P., Hinrichs, K.-U., Mollenhauer, G.,
 1006 2010. Distribution of polar membrane lipids in permafrost soils and sediments of a small
 1007 high Arctic catchment. Organic Geochemistry 41, 1130–1145.
 1008 Rohmer, M., 1993. The biosynthesis of triterpenoids of the hopane series in the Eubacteria:
 1009 A mine of new enzyme reactions. Pure and Applied Chemistry 65, 1293-1298.
 1010 Rohmer, M., Bouvier-Nave, P., Ourisson, G., 1984. Distribution of hopanoid triterpenes in
 1011 prokaryotes. Journal of General Microbiology 130, 1137–1150.
 1012 Sáenz, J.P., Sezgin, E., Schwille, P., Simons, K., 2012. Functional convergence of
 1013 hopanoids and sterols in membrane ordering. Proceedings of the National Academy of
 1014 Science 109, 14236-14240.
 1015 Schaeffer, P., Schmitt, G., Adam, P., Rohmer, M., 2008. Acid-catalyzed formation of 32,35-
 1016 anhydrobacteriohopanetetrol from bacteriohopanetetrol. Organic Geochemistry 39, 1479–
 1017 1482.
 1018 Schaeffer, P., Schmitt, G., Adam, P., Rohmer, M., 2010. Abiotic formation of 32,35-
 1019 anhydrobacteriohopanetetrol: A geomimetic approach. Organic Geochemistry 41, 1005–
 1020 1008.
 1021 Sessions, A.L., Zhang, L., Welander, P.V., Doughty, D., Summons, R.E., Newman, D.K.,
 1022 2013. Identification and quantification of polyfunctionalized hopanoids by high
 1023 temperature gas chromatography–mass spectrometry. Organic Geochemistry 56, 120–
 1024 130.
 1025 Sherry, A., Osborne, K.A., Sidgwick, F., Gray, N.D., Talbot, H.M., 2016. A temperate river
 1026 estuary is a sink for methanotrophs adapted to extremes of pH, temperature and salinity.
 1027 Environmental Microbiology Reports 8, 122-131.

1028 Simonin, P., Tindall, B., Rohmer, M., 1994. Structure elucidation and biosynthesis of 31-
 1029 methylhopanoids from *Acetobacter europaeus*. European Journal of Biochemistry 225,
 1030 765-771.

1031 Spencer-Jones, C.L., 2016. Novel concepts derived from microbial biomarkers in the Congo
 1032 System: Implications for continental methane cycling. PhD Thesis. Newcastle University,
 1033 UK.

1034 Spencer-Jones, C.L., Wagner, T., Dinga, B.J., Schefuß, E., Mann, P.J., Poulsen, J.R.,
 1035 Spencer, R.G.M., Wabakanghanzi, J.N., Talbot, H.M., 2015. Bacteriohopanepolyols in
 1036 tropical soils and sediments from the Congo River catchment area. Organic
 1037 Geochemistry doi: <http://dx.doi.org/10.1016/j.orggeochem.2015.09.003>

1038 Steart, D.C., Collinson, M.E., Scott, A.C., Glasspool, I.J., Hooker, J.J., 2007. The Cobham
 1039 lignite bed: the palaeobotany of two petrographically contrasting lignites from either side
 1040 of the Paleocene-Eocene carbon isotope excursion. Acta Palaeobotanica 47, 109-125.

1041 Stępniewska, Z., Pytlak, A., Kuźniar, A., 2013. Methanotroph activity in Carboniferous
 1042 coalbed rocks. International Journal of Coal Geology 106, 1-10.

1043 Talbot, H.M., Farrimond, P., 2007. Bacterial populations recorded in diverse sedimentary
 1044 biohopanoid distributions. Organic Geochemistry 38, 1212–1225.

1045 Talbot, H.M., Watson, D.F., Murrell, J.C., Carter, J.F., Farrimond, P., 2001. Analysis of intact
 1046 bacteriohopanepolyols from methanotrophic bacteria by reversed phase high
 1047 performance liquid chromatography - atmospheric pressure chemical ionisation - mass
 1048 spectrometry. Journal of Chromatography A 921, 175-185.

1049 Talbot, H.M., Watson, D.F., Pearson, E.J., Farrimond, P., 2003a. Diverse biohopanoid
 1050 compositions of non-marine sediments. Organic Geochemistry 34, 1353–1371.

1051 Talbot, H.M., Squier, A.H., Keely, B.J., Farrimond, P., 2003b. Atmospheric pressure
 1052 chemical ionisation reversed-phase liquid chromatography/ion trap mass spectrometry of
 1053 intact bacteriohopanepolyols. Rapid Communications in Mass Spectrometry 17, 728–737.

1054 Talbot, H.M., Summons, R.E., Jahnke, L.L., Farrimond, P., 2003c. Characteristic
 1055 fragmentation of bacteriohopanepolyols during atmospheric pressure chemical ionisation

liquid chromatography/ion trap mass spectrometry. *Rapid Communications in Mass Spectrometry* 17, 2788–2796.

Talbot, H.M., Farrimond, P., Schaeffer, P., Pancost, R.D., 2005. Bacteriohopanepolyols in hydrothermal vent biogenic silicates. *Organic Geochemistry* 36, 663–672.

Talbot, H.M., Rohmer, M., Farrimond, P., 2007a. Rapid structural elucidation of composite bacterial hopanoids by atmospheric pressure chemical ionisation liquid chromatography/ion trap mass spectrometry. *Rapid Communications in Mass Spectrometry* 21, 880-892.

Talbot, H.M., Rohmer, M., Farrimond, P., 2007b. Structural characterisation of unsaturated bacterial hopanoids by atmospheric pressure chemical ionisation liquid chromatography/ion trap mass spectrometry. *Rapid Communications in Mass Spectrometry* 21, 1613-1622.

Talbot, H.M., Summons, R.E., Jahnke, L.L., Cockell, C.S., Rohmer, M., Farrimond, P., 2008. Cyanobacterial bacteriohopanepolyol signatures from cultures and natural environmental settings. *Organic Geochemistry* 39, 232–263.

Talbot, H.M., Handley, L., Spencer-Jones, C.L., Dinga, B.J., Schefuß E., Mann, P.J., Poulsen, J.R., Spencer, R.G.M., Wabakanghanzi, J.N., Wagner, T., 2014. Variability in aerobic methane oxidation over the past 1.2 Myrs recorded in microbial biomarker signatures from Congo fan sediments. *Geochimica et Cosmochimica Acta* 133, 387-401.

van Dongen, B.E., Talbot, H.M., Schouten, S., Pearson, P.N., Pancost, R.D., 2006. Well preserved Palaeogene and Cretaceous biomarkers from the Kilwa area, Tanzania. *Organic Geochemistry* 37, 539–557.

van Winden, J.F., Talbot, H.M., Kip, N., Reichart, G.-J., Pol, A., McNamara, N.P., Jetten, M.S.M., Op den Camp, H.J.M., Sinninghe Damsté, J.S., 2012a. Bacteriohopanepolyol signatures as markers for methanotrophic bacteria in peat moss. *Geochimica et Cosmochimica Acta* 77, 52–61.

1082 van Winden, J.F., Talbot, H.M., De Vleeschouwer, F., Reichart, G.J., Sinninghe Damsté,
 1083 J.S., 2012b. Variation in methanotroph-related proxies in peat deposits from Misten Bog,
 1084 Hautes-Fagnes, Belgium. *Organic Geochemistry* 53, 73-79.

1085 Wagner, T., Kallweit, W., Talbot, H.M., Mollenhauer, G., Boom, A., Zabel, M., 2014.
 1086 Microbial biomarkers support organic carbon transport from Amazon wetlands to the shelf
 1087 and deep fan during recent and glacial climate conditions. *Organic Geochemistry* 67, 85-
 1088 98.

1089 Wakeham, S.G., Amann, R., Freeman, K.H., Hopmans, E., Jørgensen, B.B., Putnam, I.F.,
 1090 Schouten, S., Sinninghe Damsté, J.S., Talbot, H.M., Woebken, D., 2007. Microbial
 1091 ecology of the stratified water column of the Black Sea as revealed by a comprehensive
 1092 biomarker study. *Organic Geochemistry* 38, 2070-2097.

1093 Watson, D.F., 2002. Environmental Distribution and Sedimentary Fate of Hopanoid
 1094 Biological Marker Compounds. PhD Thesis, University of Newcastle, UK.

1095 Welander, P.V., Summons, R.E., 2012. Discovery, taxonomic distribution, and phenotypic
 1096 characterization of a gene required for 3-methylhopanoid production. *Proceedings of the*
 1097 *National Academy of Science, USA* 109, 12905-12910.

1098 Welander, P.V., Hunter, R.C., Zhang, L., Sessions, A.L., Summons, R.E., Newman, D.K.,
 1099 2009. Hopanoids play a role in membrane integrity and pH homeostasis in
 1100 *Rhodopseudomonas palustris* TIE-1. *Journal of Bacteriology* 191, 6145-6156.

1101 Xu, Y., Cooke, M.P., Talbot, H.M., Simpson, M.E., 2009. Bacteriohopanepolyol signatures of
 1102 bacterial populations in Western Canadian soils. *Organic Geochemistry* 40, 79–86.

1103 Zhu, C., Talbot, H.M., Wagner, T., Pan, J., Pancost R.D., 2010. Intense aerobic methane
 1104 oxidation in the Yangtze estuary: A record from 35-aminobacteriohopanepolyols in
 1105 surface sediments. *Organic Geochemistry* 41, 1056-1059.

1106 Zhu, C., Talbot, H.M., Wagner, T., Pan, J.-M., Pancost, R.D., 2011. Distribution of hopanoids
 1107 along a land to sea transect: implications for microbial ecology and the use of hopanoids
 1108 in environmental studies. *Limnology and Oceanography* 56, 1850-1865.

Figure legends

Figure 1. (a) Partial APCI mass chromatograms showing base peak ions of individual BHPs which do not contain a nitrogen atom identified via LCMSⁿ. (b) Partial EI mass chromatograms including m/z 191 and 205 fragments (A/B rings) and characteristic D/E +side chain fragments for BHPs identified via GCMS. See appendix for structures. Data from sample depth 11.95 cm (laminated lignite; Table 1).

Figure 2. Partial APCI mass chromatograms showing base peak ions of individual BHPs identified via LCMSⁿ which contain a nitrogen atom. See appendix for structures. Data from sample depth 115.65 cm (blocky lignite; Table 1.)

Figure 3. EI and APCI MS² mass spectra (respectively) of peracetylated derivatives of (a and b) AnhydroBHT, (c and d) proposed “side chain methylated” AnhydroBHT and (e and f) proposed “side chain methylated” 3-methyl-AnhydroBHT (note this compound co elutes with BHT and anhydroBHpentol by GCMS as indicated by the D/E+side chain fragments m/z 493 and 449 respectively; underlined ions in panel e are consistent with the proposed structure). Position of “side-chain methylation” at C-31 in structures shown in parts c-f is tentative (cf. Simonin et al., 1994; Nytoft, 2011). For identification of peaks see Figure 1. Key: Ac = -COCH₃; # indicates peak related to aminotriol (**If**; Figure 2). Spectra taken from sample depth 11.95 cm, (laminated lignite, Table 1).

Figure 4. APCI MS² spectra of peracetylated derivatives of (a) Aminotriol [**If**], (b) Aminotetrol [**Ig**], (c) Aminopentol [**Ih**], (d) anhydroaminotriol (**li**; cf. Eickhoff et al., 2014) (e) proposed 31-oxo-35-aminobacteriohopane-32,33,34-triol [**Ik**] and (f) proposed 32-oxo-35-aminobacteriohopane-33,34 diol [**Ij**]. For identification and relative retention times of peaks see Figure 2. Key: Ac = -COCH₃; * indicates loss of 42 Da i.e. partial loss of acetylated OH group as ketene COCH₂; (Talbot et al., 2003b); # indicates ions arising from fragmentation of co-eluting parent ion m/z 669, Fig. 1). Data from sample depth 115.65 cm (blocky lignite; Table 1.)

Figure 5. APCI MS² and EI mass spectra (respectively) of peracetylated derivatives of (a and b) proposed 31-oxo-bacteriohopane-32,33,34,35-tetrol [**le**], (c) APCI MS² spectrum of AnhydroBHpentol (isomer i; cf. Talbot et al., 2005) and (d) EI mass spectrum of AnhydroBHpentol (co-eluting with BHT [**lc**] and “side chain methylated” 3-methyl-anhydroBHT [**lllb**]). For identification of peaks see Figure 1. Data from sample depth 11.95 cm (laminated lignite; Table 1).

Figure 6. Plots of (a) $\delta^{13}\text{C}$ values of bulk OM, (b) $\delta^{13}\text{C}$ values of C₂₉ (circles) and C₃₁ (diamonds) hopanes, (c) total biohopanoids as a proportion of total BHPs and (d-h) individual polyfunctionalised biohopanoids as a proportion of total biohopanoids in the Cobham lignite sequence. Open circles indicate 5 samples from within the onset of the CIE (54.4 – 56.6 cm), black circles indicate all other samples. Shaded grey bars indicate clay horizons including lignite with clay laminae in the middle section (Table 1). All isotope data from Pancost et al. (2007) and lithology after Collinson et al. (2003) and Steart et al. (2007).

Figure 7. Plots of (a) $\delta^{13}\text{C}$ values of bulk OM, (b) $\delta^{13}\text{C}$ values of C₂₉ (circles) and C₃₁ (diamonds) hopanes, (c) relative abundance of total geohopanoids as % of total BHPs and (d-h) selected known and novel polyfunctionalised hopanoid transformation products as a proportion of total geohopanoids in the Cobham Lignite sequence. Open circles indicate 5 samples from within the onset of the CIE (54.4 – 56.6 cm), black circles indicate all other samples. Shaded grey bars indicate clay horizons including lignite with clay laminae in the middle section (Table 1). All isotope data from Pancost et al. (2007) and lithology from Collinson et al. (2003) and Steart et al. (2007).

Figure 8. Average relative abundance of all BHPs in Cobham lignite sequence (a) blocky lignite [67.5 – 135 cm], (b) clay layer plus uppermost laminated lignite and lowest blocky lignite [57.2-66.8 cm], (c) Onset of carbon isotope excursion [CIE] in laminated lignite [54.45 – 56.6 cm] and (d) lower laminated lignite and sample from sand/mud unit [-1.5 – 54.15 cm].

1161 White bars indicate compounds containing a nitrogen atom, black bars compounds not
1162 containing nitrogen. See Appendix for structures.

1163

1164

1165 **Table 1.** Sample depth in sequence, lithology, bulk carbon isotope ratio values (‰) and relative abundance (%) of individual BHPs
 1166 from LCMS analysis and biomarker ratios in the Cobham Lignite.

1167

Level (cm)	Lithology ^a	$\delta^{13}\text{C}$ TOC ^b	Biohopanoids				Polyfunctionalised geohopanoids/Novel products									Ratios	
			lc	lf	lg	lh	la	la'	lb	lllb	ld	le	li	lj	lk	654/714 ^e	lf/li
135	Blocky Lignite	nm ^c	- ^d	2.8	-	-	60.1	-	11.5	-	4.5	1.9	13.5	5.7	-	5.0	
131.4	Blocky Lignite	-26.82	-	-	-	-	100	-	-	-	-	-	-	-	-		
118.65	Blocky Lignite	-26.93	31.4	23.8	21.1	-	16.3	-	1.8	-	-	-	5.6	-	-	0.4	1.1
115.65	Blocky Lignite	nm	4.1	8.3	4.3	4	41.9	2.3	3.9	0.5	5.2	5.5	8.7	5.3	6	1.2	1.9
102.4	Blocky Lignite	-27.33	1.6	3.6		-	62		7.7	1.3	5	2.7	8.8	4	3.3	2.6	
85.9	Blocky Lignite	-26.14	1.9	3.1	0.3	0.5	60	2.7	8.8	1.8	7.5	3.1	5.8	2.2	2.3	2.0	10.3
75.2	Blocky Lignite	-26.77	1.5	5	1.5	0.7	51.8	-	3.1		2.6	6	14.3	6.3	7.2	3.1	3.3
73.95	Blocky Lignite	-26.82	1.8	5.8	0.4	0	46.2	-	6.2	1.4	5.1	5	17.2	7.5	3.4	3.2	14.5
70.3	Blocky Lignite	nm	1.3	7	2.8	1.5	45.8	-	5.4		1	5.2	14.4	6.1	9.5	2.2	2.5
69.75	Blocky Lignite	nm		6.8	2.1	-	58	-	9.7			3.5	15.9	1.8	2.2	2.5	3.2
69.35	Blocky Lignite	-26.81	1.2	1.2	0.4	0.2	61.3	3.9	9.8	1.7	5.8	6.6	4.5	2.2	1.2	3.9	3.0
68.85	Blocky Lignite	nm	0.7	1.6	0.7	0.2	62.2	4.1	9.6	2.1	5.6	4.4	4.3	1.5	3	2.9	2.3
68.4	Blocky Lignite	nm	1.6	2.1	1	0.2	64.8	4	9.5	2.1	5.2	3.9	4	1.2	0.4	2.1	2.1
67.5	Blocky Lignite	nm	2.6	11.3	13.4	0.6	39.4	4.4	8.9	2.3	4.6	3.4	6.4	1.5	1.2	0.7	0.8
66.8	Blocky Lignite with clay layers	-24.17	7.5	22.6	48.2	-	14.4	-	4.1	0.5	0.7	0.9	1.1	-	-	0.2	0.5
65.3	Clay	-24.83	42.6	29.6	27.8	-	-	-	-	-	-	-	-	-	-	0.2	1.1
58.75	Clay	-25.45	29.1	28.4	33.1	-	6	-	-	-	-	-	3.4	-	-	0.3	0.9
57.2	Laminated Lignite with clay layers	-25.75	14.6	43.1	35.9	-	5.1	-	-	-	-	-	1.3	-	-	0.2	1.2
56.6	Laminated Lignite	-26.97	2	5.2	1.6	0.7	50.3	-	7.6	0.8	6.5	3.7	11.9	5.3	4.4	2.5	3.3
55.9	Laminated Lignite	-26.72	1.2	5.4	0.9	0.8	44.5	-	6	0.7	5.2	3.8	12.6	8	10.9	2.5	6.0
55.3	Laminated Lignite	-27.10	-	5.2	-	-	39.9	-	-	-	-	7.8	29.7	8.6	8.8	5.9	
54.85	Laminated Lignite	-27.16	-	4	0.9	0.8	44.7	-	3.6	-	3	5	15.8	9.5	10.5	4.1	4.4

54.45	Laminated Lignite	-27.01	-	2.5		-	42.4	-	-	-	-	-	26	17.9	11.2	10.7	
54.15	Laminated Lignite	-26.01	-	11.7	5.3	-	70.8	-	-	-	-	-	12.2	-	-	1.2	2.2
43.3	Laminated Lignite	-25.51	1.4	14.2	4.8	-	43.7	-	6.8	0.6	1.7	2.1	20.4	3.1	1.2	1.6	3.0
42.4	Laminated Lignite	-25.20	32.9	-	-	-	50	-	-	-	-	-	17.1	-	-		
41.5	Laminated Lignite	-26.01	1.2	9.3	1.5	-	52.7	-	4.9	1.5	1.6	1.6	19.8	3.8	2.1	2.3	6.2
40.65	Laminated Lignite	-25.28	-	8.3	-	-	45.9	-	-	-	-	-	45.8	-	-	5.7	
39.8	Laminated Lignite	-26.10	1.5	10.1	0.9	-	53.5	-	6.1		5.7	1.5	17.6	2.4	0.7	1.9	11.2
36.1	Laminated Lignite	-25.21	-	7.3	0.6	-	44.4	-	8.3	1.4	5.1	1.9	22.5	5.9	2.6	3.3	12.2
23.05	Laminated Lignite	-25.62	2.9	4.1	0.5	0.6	66.5	2.6	8.6	1.1		2.9	7.3	2	0.9	2.0	8.2
16.5	Laminated Lignite	-25.83	2.1	4.2	0.5	0.2	59.9	2.3	10.6	1.3	4.4	4.4	7.5	2.1	0.5	2.0	8.4
11.95	Laminated Lignite	-26.41	1.8	2.5	0.1	-	60.3	3.5	12.6	1.9	4.6	3.5	7.6	1.4	0.2	3.2	25.0
4.65	Laminated Lignite	-24.77	4.5	1.8	14.3	-	56.5	3.3	9.7	1.2	4.2	3	0.7	0.8	-	0.6	0.1
-1.5	Sand/mud	-25.62	9.6	7.3	20.4	-	45.5	-	10	3.5	2.7	-	1	-	-	0.3	0.4

1168

1169

1170 ^a Detailed description of the lithologies can be found in Collinson et al. (2003) and Steart et al. (2007)

1171 ^b Values from Pancost et al. (2007)

1172 ^c nm =not measured

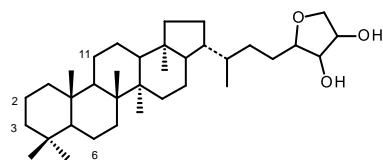
1173 ^d - indicates compound below detection limit.

1174 ^e ratio calculated from raw peak area before adjustment of the anhydroaminotriol value (see section 2.3).

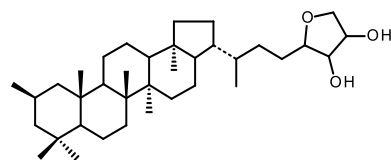
1175

1176 **Appendix 1.**

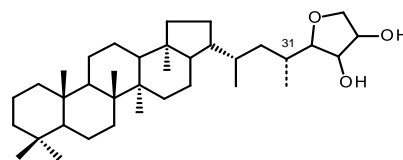
1177 Structures referred to throughout the text and common abbreviated names.



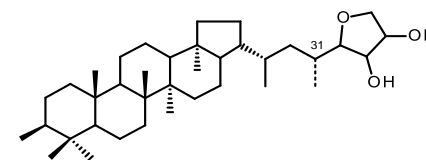
Ia
AnhydroBHT



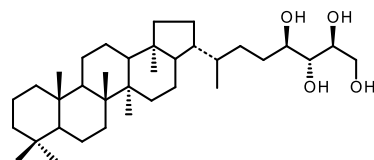
IIa
2-methyl-AnhydroBHT



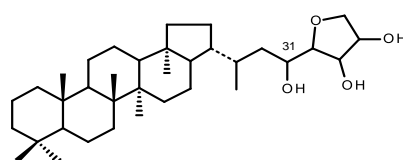
Ib
31-methyl-AnhydroBHT^a



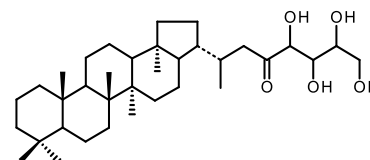
IIIb
3,31-methyl-AnhydroBHT^a



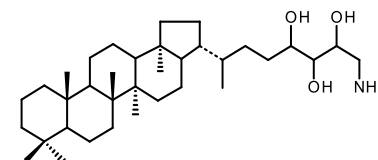
Ic
Bacteriohopanetetrol (BHT)



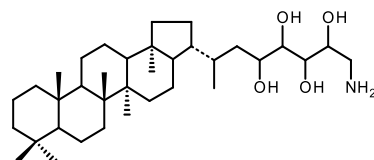
Id
AnhydroBHpentol



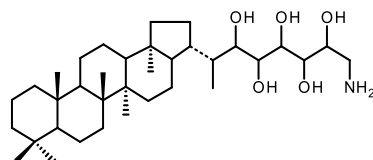
Ie
31-oxo-BHT^b



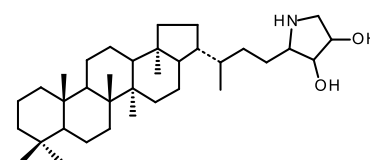
If
Aminotriol



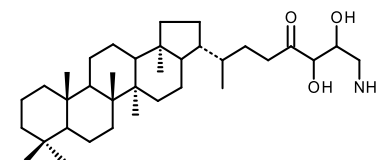
Ig
Aminotetrol



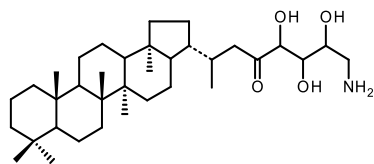
Ih
Aminopentol



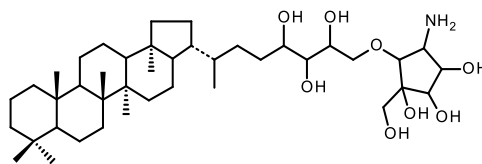
Ii
Anhydroaminotriol



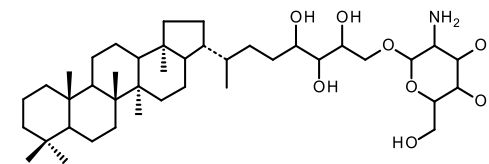
Ij
32-oxo-35-Aminodiol^b



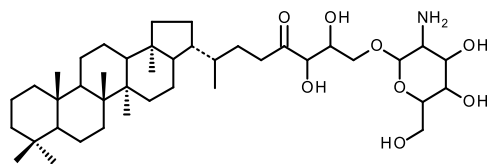
lk
31-oxo-35-Aminotriol^b



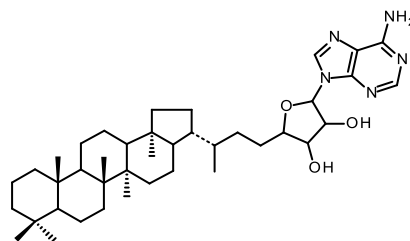
lm
BHT cyclitol ether



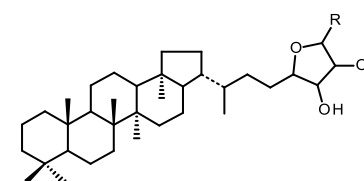
ln
BHT glucosamine



lo
32-oxo-bateriohopanetriol glucosamine



lp
Adenosylhopane



lq
Adenosylhopane-type^c
(R = unknown)

1178

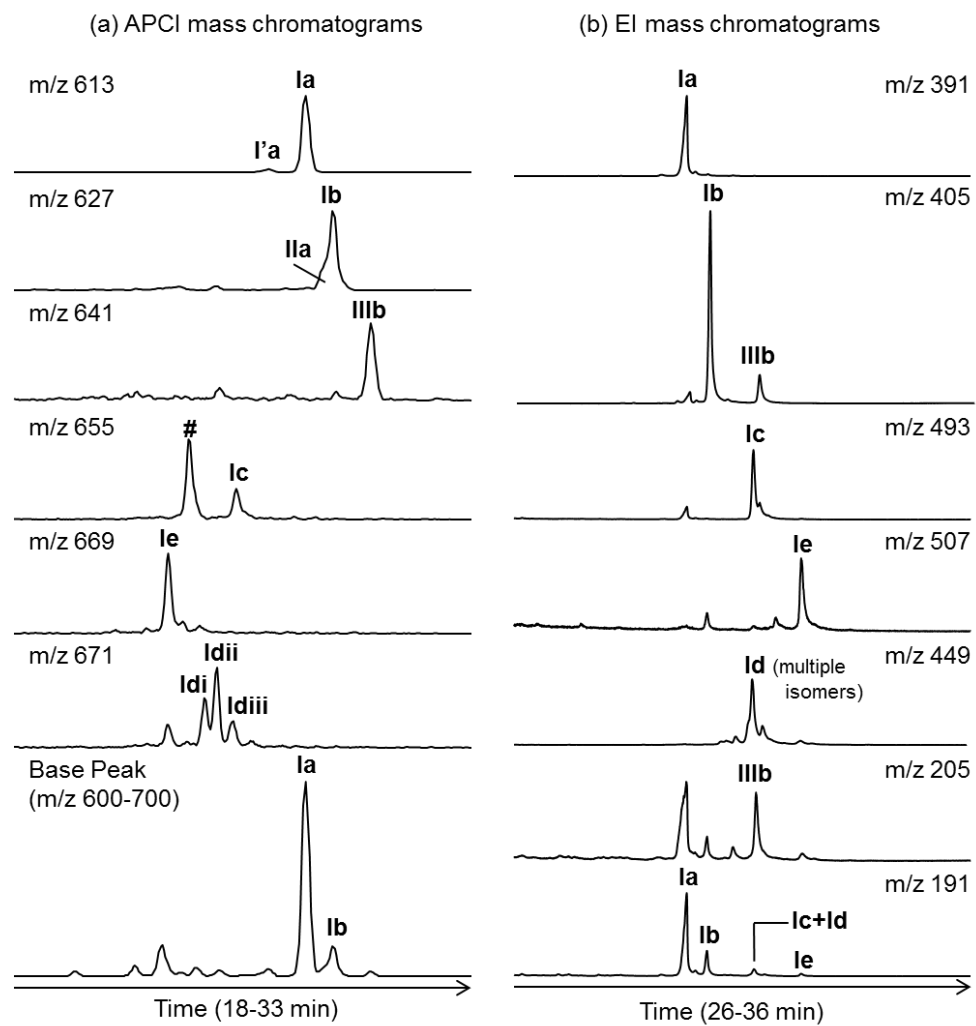
1179 ^a position of methylation at C-31 is tentative but limited to the side chain based on EI spectra (Fig. 3) and indicated at C-31 based
1180 on previous studies (Simonin et al., 1994; Nytoft, 2011)

1181 ^b location of ketone is tentative but is limited to the side chain in **le** based on EI spectrum (Fig. 5)

1182 ^c terminal group structure (R) unknown but can be differentiated from **lp** based on APCI base peak ion and MS² spectrum (Cooke
1183 et al., 2008a; Rethemeyer et al., 2010).

1184

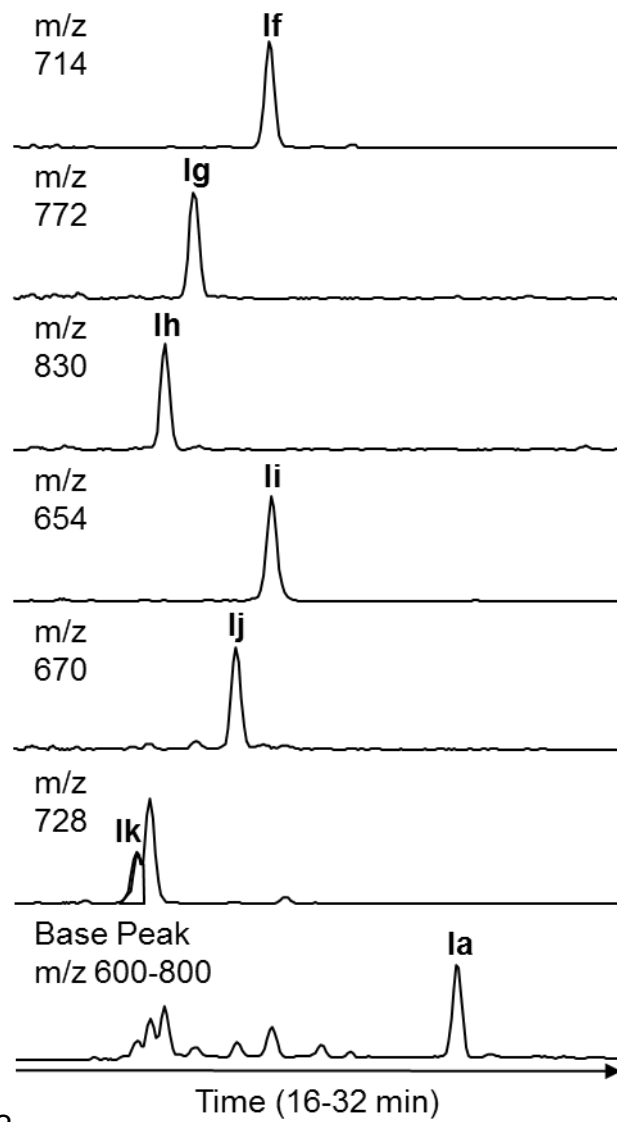
1185



1186

1187 Figure 1

1188



1189 Figure 2

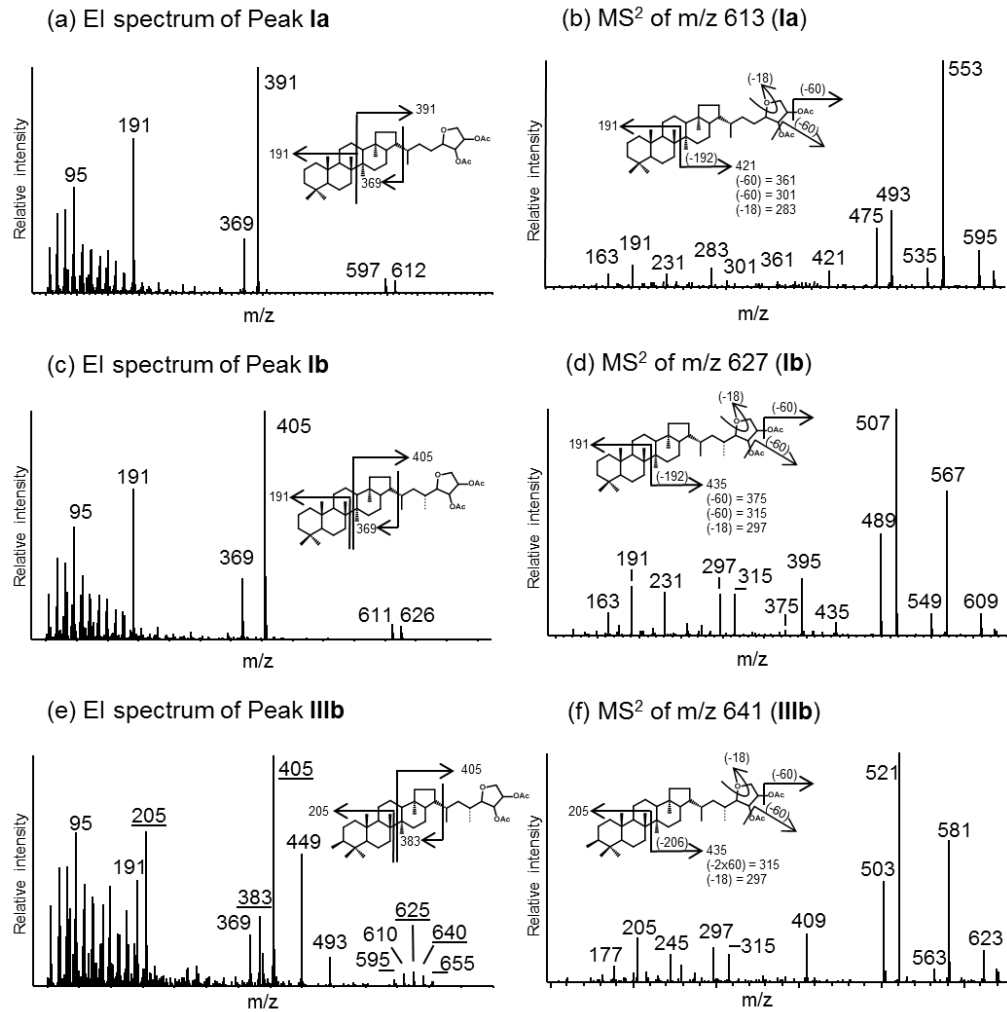


Figure 3.

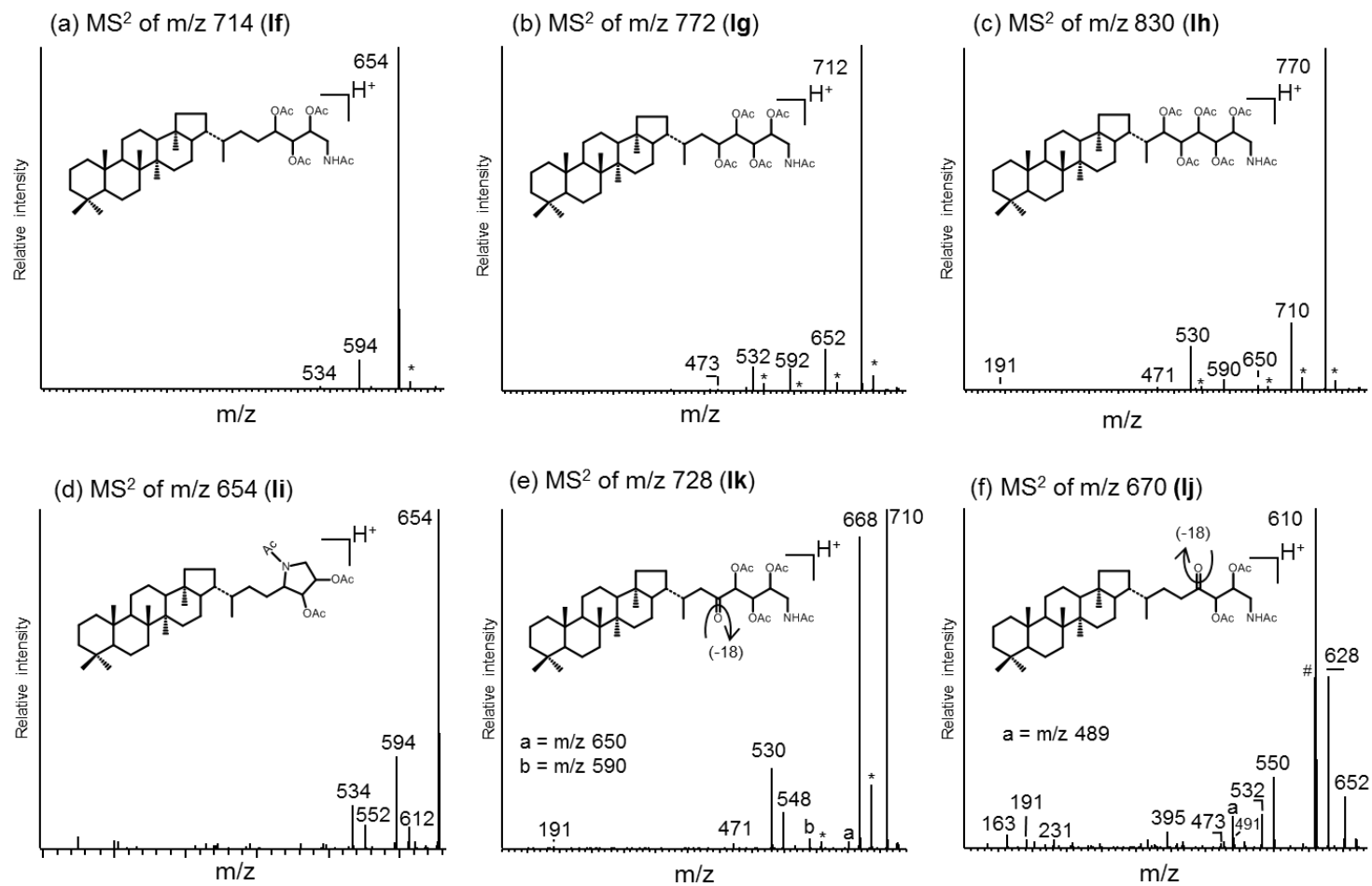
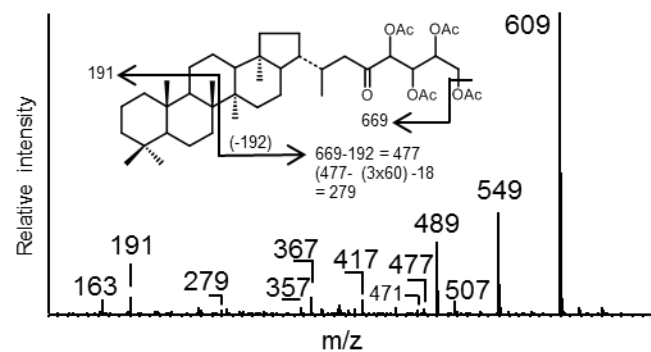
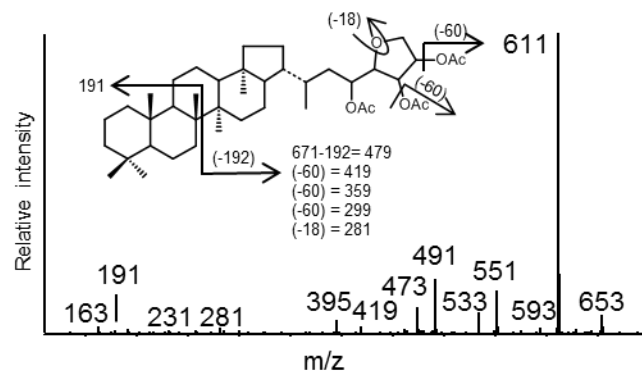


Figure 4.

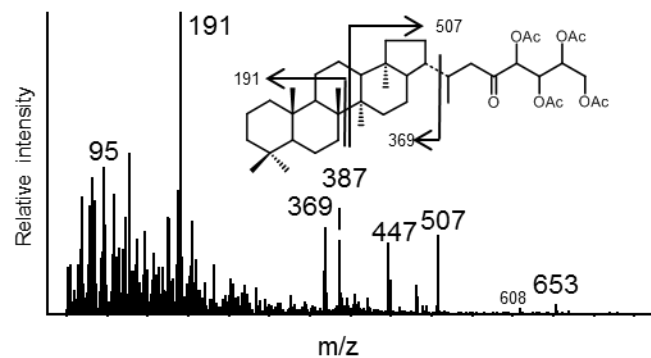
(a) MS² of m/z 669 (peak **le**)



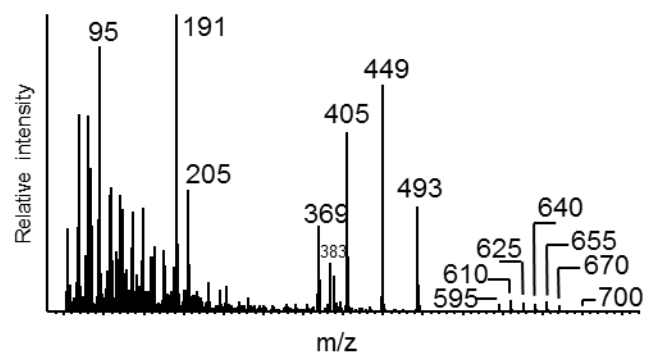
(c) MS² of m/z 671 (peak **ldi**)



(b) EI MS of peak **le**



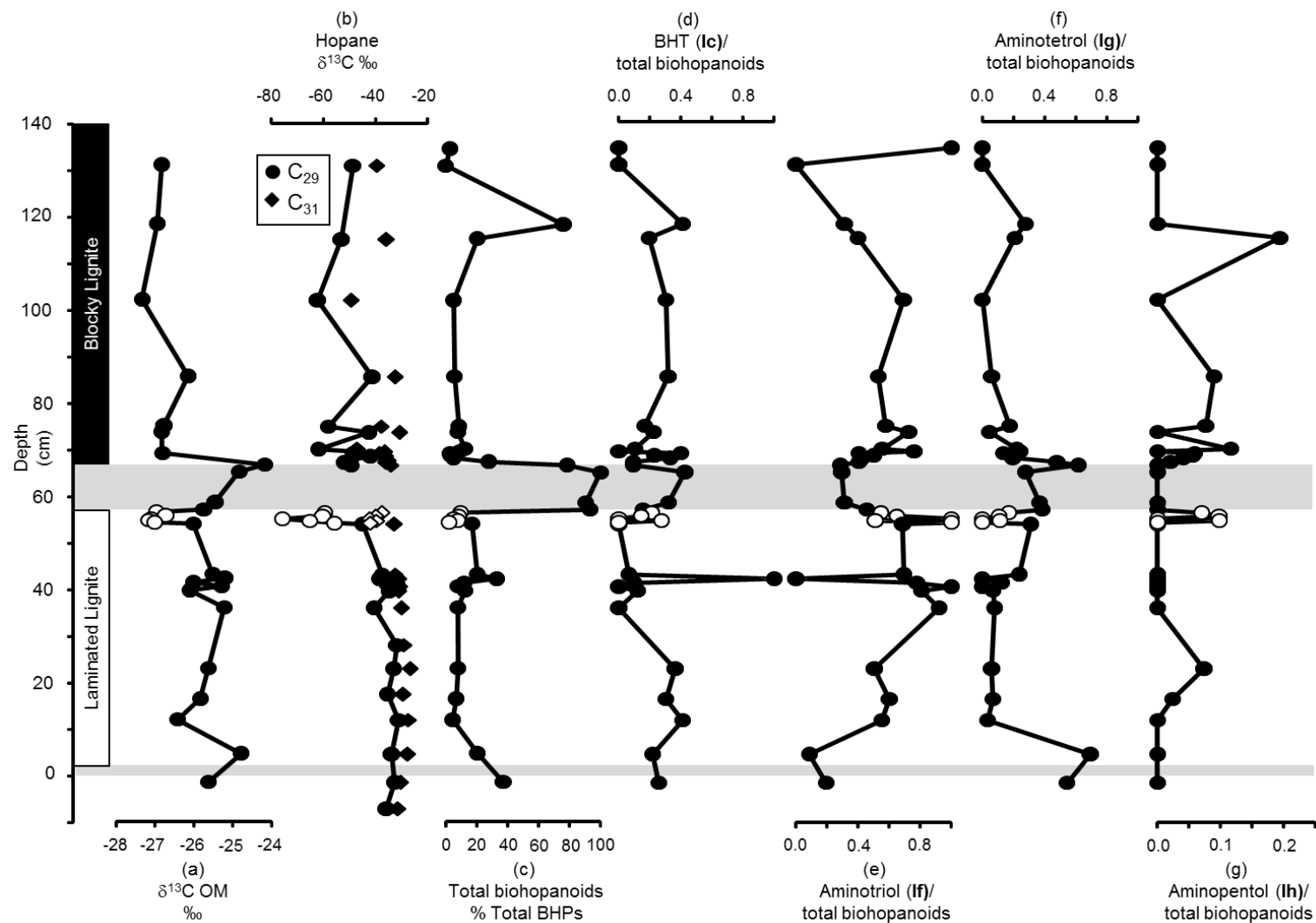
(d) EI MS of peak (**lc+ld+lllb**)



1197

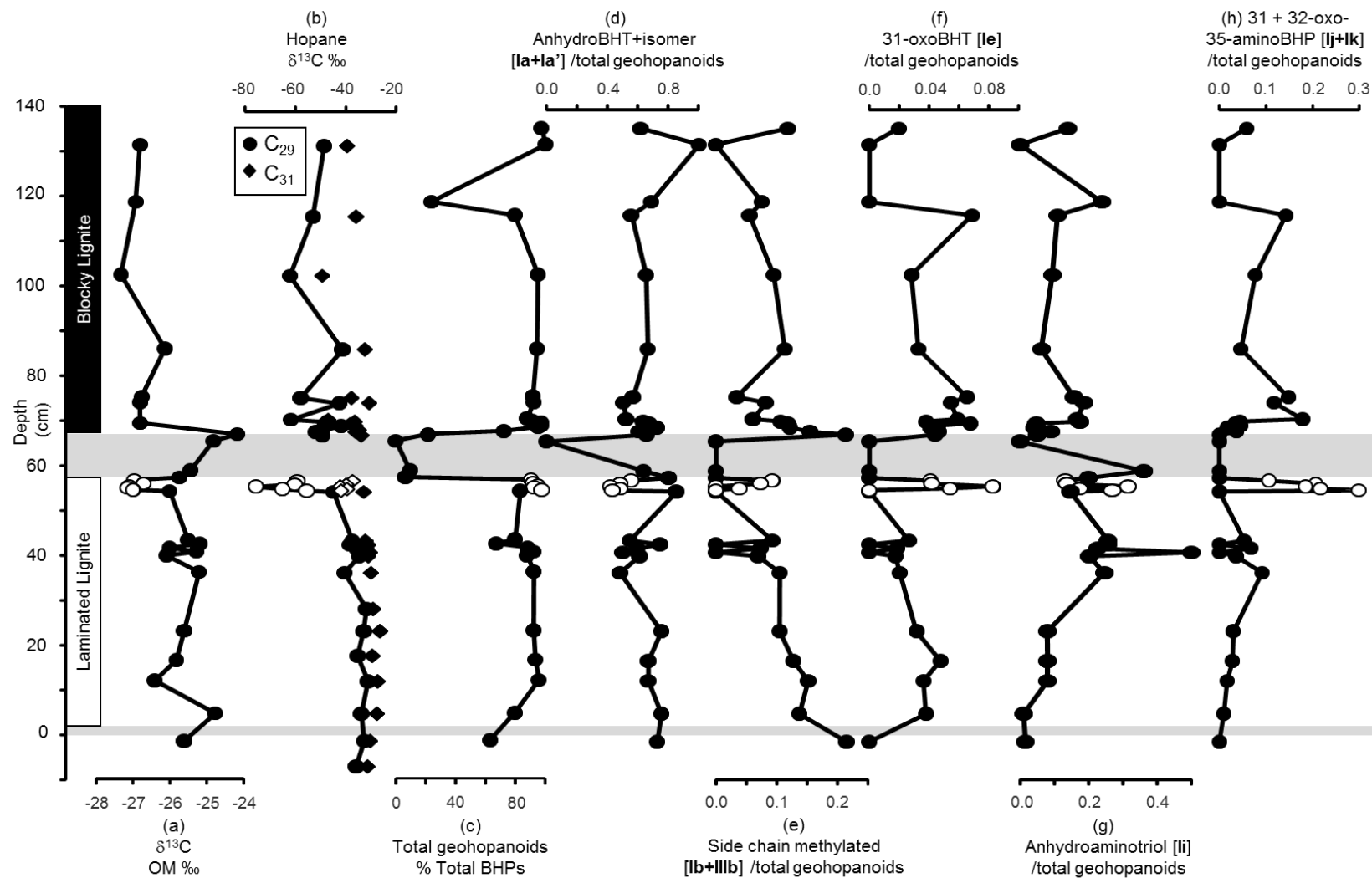
1198 Figure 5.

1199



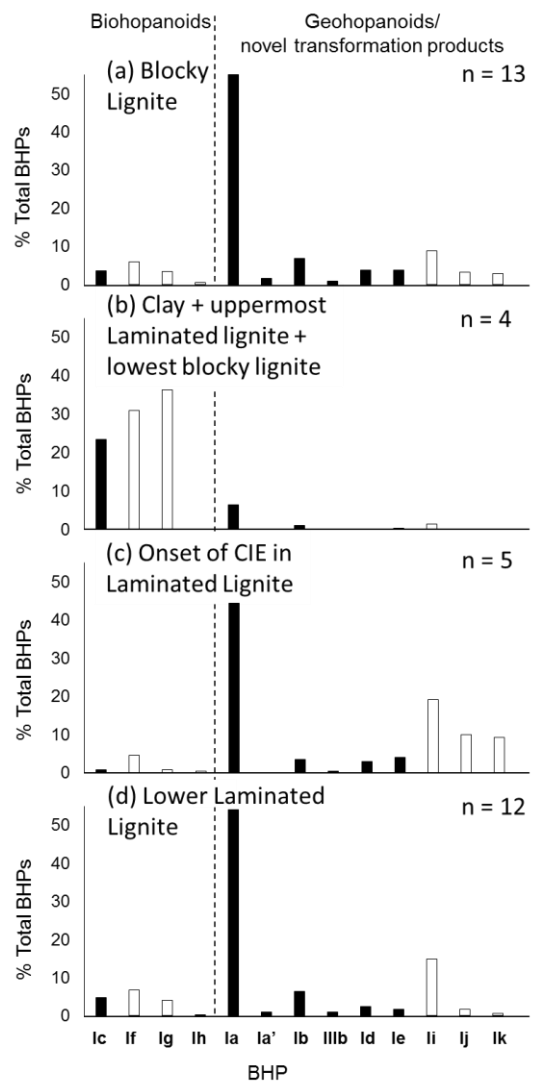
1200

1201 Figure 6.



1202

1203 Figure 7.



1204

1205 Figure 8.